

ANALYTICAL PERFORMANCE EVALUATION OF AN OPTICAL
WIRELESS COMMUNICATION SYSTEM WITH OOK AND
M-ARY PPM MODULATION IN THE PRESENCE OF
ATMOSPHERIC EFFECTS



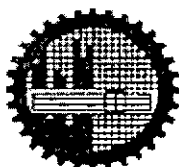
A Thesis submitted to the Department of Electrical and Electronic Engineering,
Bangladesh University of Engineering and Technology (BUET),
Dhaka –1000, Bangladesh

in partial fulfilment of the requirements for the degree of Master of Science in
Engineering (Electrical and Electronic Engineering).

By

T.M. Fahim Amin

*Under the supervision of
Professor Dr. S. P. Majumder*



Department of Electrical and Electronic Engineering
Bangladesh University of Engineering and Technology
Dhaka, Bangladesh.

November 2007



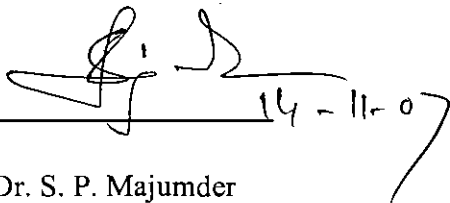
#104533#

DECLARATION

This is declared that the thesis "Analytical Performance Evaluation of an Optical Wireless Communication System with OOK and M-ary PPM Modulation in the Presence of Atmospheric Effects" presented here is an outcome of the investigation carried out by the undersigned student under the supervision of Professor Dr. S. P. Majumder, Department of Electrical and Electronic Engineering, BUET.

This work has been done by the student undersigned and it has not been submitted elsewhere for the award of any degree or diploma.

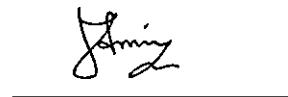
Countersigned



14-11-07

Dr. S. P. Majumder
Professor and Head
Department of EEE, BUET
Dhaka-1000
Bangladesh

Signature of the student



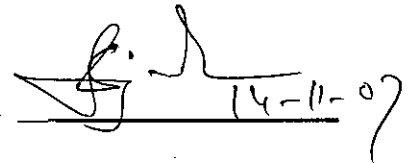
T. M. Fahim Amin

The Thesis "ANALYTICAL PERFORMANCE EVALUATION OF AN OPTICAL WIRELESS COMMUNICATION SYSTEM WITH OOK AND M-ARY PPM MODULATION IN THE PRESENCE OF ATMOSPHERIC EFFECTS" submitted by T.M. Fahim Amin , Roll No. 040506222, session "April 2005" to the Department of Electrical and Electronic Engineering, Bangladesh University of Engineering and Technology, Dhaka, has been accepted as satisfactory in partial fulfilment of the requirements for the for the degree of Master of Science in Engineering (Electrical and Electronic Engineering).

Board of Examiners

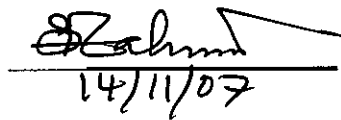
1. Dr. Satya Prasad Majumder
Professor and Head
Department of EEE
BUET, Dhaka-1000
Bangladesh.
(Supervisor)

Chairman


14-11-07

2. Dr. Md. Saifur Rahman
Professor
Department of EEE
BUET, Dhaka-1000
Bangladesh

Member


14/11/07

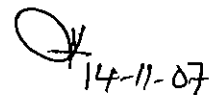
3. Dr. Md. Shah Alam
Associate Professor
Department of EEE
BUET, Dhaka-1000
Bangladesh.

Member


14/11/07

4. Engr. Md. Abdul Moqaddem
(M. Sc. Engg., BUET)
DGM, Teletalk Bangladesh Ltd.
House no. 41, Road-27, Block-A
Banani, Dhaka.

Member (External)


14-11-07

ACKNOWLEDGEMENT

This project is accomplished under the supervision of Dr. Satya Prasad Majumder, Professor and Head, Department of Electrical and Electronic Engineering, Bangladesh University of Engineering and Technology (BUET), Dhaka. It is a great pleasure to express the author's indebtedness gratitude and profound respect to his supervisor for the supervisor's consistent guidance, relentless encouragement, helpful suggestions, constructive criticism and endless patience throughout the progress of this research. The successful completion of this thesis would not have been possible without his persistent motivation and continuous guidance.

The author is also grateful to Md. Adnan Momin, Additional General Manager, Service Network, Technical Division, Grameen Phone Ltd. and also Mr. Anisul Mazid, Deputy Chief Engineer, Service Network, Technical Division, Grameen Phone Ltd. for their consistent support in completing this work successfully.

The author is also indebted to the librarian and other staffs of the Department of EEE for their help and cooperation in completing the project.

Finally, all praises to Allah, the most gracious benevolent, without Whose help this work would not have been possible.

ABSTRACT

Optical wireless communication—both in space and outdoor and indoor terrestrial applications is rapidly becoming a major feature of modern life. It has been researched widely in recent years due to the increasing interest in laser satellite-ground links and urban optical wireless communication. The major sources of performance degradation have been identified as the spatial, angular, and temporal spread of the propagating beam when the propagation channel is multiscattering, resulting in reduced power reception and inter-signal interference, as well as noise due to receiver circuitry and background illumination. In this thesis a theoretical analysis is provided to evaluate the performance of optical On Off keying (OOK) and M-ary Pulse Position Modulation (MPPM) transmission link taking into account the effect of laser phase noise, spontaneous emission noise of the optical amplifier of the link and other heat noises arising due to beating of the signal with spontaneous noise at the photodetector output. The analytical expressions of bit error rate (BER) of an optical wireless link in the presence of atmospheric scintillation using OOK and M-ary PPM modulation schemes is derived and the analysis is extended for a multiscattering channel considering a fixed scintillation variance. Using these expressions the performance of direct detection OOK and MPPM systems on the presence of atmospheric scintillation and also for mutiscattering channel are evaluated. Computed results show that in the presence of both atmospheric scintillation and multiscattering effect higher order PPM offers better performance than OOK at a given BER.

CONTENTS

	Page
A. Declaration	(i)
B. Approval	(ii)
C. Acknowledgement	(iii)
D. Abstract	(iv)
E. Contents	(v)
F. Lists of Figures	(viii)
G. Lists of Tables	(x)
H. List of Important Abbreviation	(xi)

CHAPTER ONE *General Introduction*

1.1 General perspective	1
1.2 Advantage of Optical Wireless Communication	3
1.3 Brief History of optical Communication System	4
1.4 Recent Optical Wireless Communication Systems	5
1.4.1 Indoor applications	5
1.4.2 Outdoor applications	9
1.5 Purpose and Position of This study	11
1.6 objective of this Study	12

CHAPTER TWO *Basic Knowledge of optical Wireless Communication Systems*

2.1	Comparison between Lightwave and Radio Media	13
2.2	Optical Wireless link Design	15
2.3	IM/DD Channels	16
2.4	Design of Power Efficient Links	19
2.5	Major Components of Optical wireless link	19
2.5.1	Optical Sources	20
2.5.1.1	Light Emitting Diode (LED)	20
2.5.1.2	Laser	20
2.5.2	Optical Detectors	22
2.5.2.1	PIN Diode	22
2.5.2.2	Avalanche Photo Diode (APD)	22
2.6	Optical Transmitters and Eye Safety	23

CHAPTER THREE *Performance Analysis of OOK and M-PPM System in Direct Detection Optical Wireless Communication without Atmospheric Effects*

3.1	Introduction	26
3.2	System Receiver Model	27
3.3	Input Signal to OOK/PPM receiver	28
3.4	Receiver Output Statistics	28
3.5	Analysis of OOK System without Atmospheric Effects	31
3.6	Analysis of M-PPM System without Atmospheric Effects	33

CHAPTER FOUR *Performance Analysis of OOK and M-PPM System in Direct Detection Optical Wireless Communication in the Presence of Atmospheric Effects*

4.1 Introduction	35
4.2 Performance Analysis with Atmospheric Scintillation	35
4.3 Performance Analysis with Atmospheric Scintillation and Multiscattering	38

CHAPTER FIVE *Results and Discussion*

5.1 Introduction	43
5.2 Results and Discussion	43

CHAPTER SIX *Conclusion*

6.1 Conclusion	61
6.2 Further Scope of Works	62

References	63
------------	----

Appendices

APPENDIX A: Simplification of Probability Bit Error Rate (BER) for ON OFF Keying	71
APPENDIX B: Simplification of Probability Bit Error Rate (BER) for M-PPM	73
APPENDIX C: HERMITE POLYNOMIAL	79

List of Figures

1.1	Wired backbone and wireless access networks	2
1.2	Integration of radio and optical communication	3
1.3	An example of an IrDA	6
1.4	The IrDA protocol stack	6
1.5	IrDA optical geometry	6
1.6	An example of an IEEE 8.2.11 network with infrared transmission	9
1.7	Examples of an outdoor optical wireless communication system	10
2.1	Classification of simple infrared links according to the degree of directionality of the transmitter (T) and receiver (R) and whether the link rely upon the existence of a LOS path between them	16
2.2	Modeling link as a baseband filter, time-invariant system having impulse response $h(t)$, with signal-independent, additive noise $N(t)$	17
2.3	Basic Optical Wireless Communication Link	20
2.4	The three keys transition process involved in laser action. The open circle represents the initial state of the electron and the heavy dot represents the final state. Incident photons are shown on the left of each diagram and emitted photons are shown on the right.	21
3.1	A receiver model for optical OOK and PPM system	27
4.1	Probability distribution functions of scatter angle	39
5.1	Performance of optical OOK and M-PPM receiver without atmospheric effects	45
5.2	Performance of optical OOK and M-PPM receiver in the presence of atmospheric scintillation ($\sigma_s^2=0.001$)	46
5.3	Performance of optical OOK and M-PPM receiver in the presence of atmospheric scintillation ($\sigma_s^2=0.005$)	47

5.4	Performance of optical OOK and M-PPM receiver in the presence of atmospheric scintillation ($\sigma_s^2=0.01$)	48
5.5	Performance of optical OOK and M-PPM receiver in the presence of atmospheric scintillation ($\sigma_s^2=0.03$)	49
5.6	Performance of optical OOK and M-PPM receiver in the presence of atmospheric scintillation ($\sigma_s^2=0.05$)	50
5.7	Performance of optical OOK and M-PPM receiver in the presence of lower atmospheric scintillation	51
5.8	Performance of optical OOK and M-PPM receiver in the presence of higher atmospheric scintillation	52
5.9	Penalty as a function of variance of scintillation	53
5.10	Plots of BER vs Average Photon Count/bit for no scattered fields	55
5.11	Plots of BER vs Average Photon Count/bit with scattered fields (N=1)	56
5.12	Plots of BER vs Average Photon Count/bit with scattered fields (N=2)	57
5.13	Plots of BER vs Average Photon Count/bit with scattered fields (N=3)	58
5.14	Plots of BER vs Average Photon Count/bit for different no of scattered fields	59
5.15	Penalty as a function of no. of scattered fields	60

List of Tables

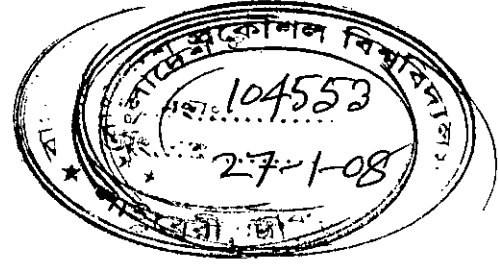
1.1	Signaling rate and pulse duration specifications of IrDA 1.4	7
2.1	Comparison between radio and IM/DD optical wireless systems	14
2.2	Comparison between LED's and LD's	23
5.1	Nominal Parameters of Optical Wireless Communication link	44

List of Important Abbreviation

OOK	On Off Keying
MPPM	M-ary Pulse Position Modulation
BER	Bit Error Rate
APD	Avalanche Photodiode
EMI	Electro-Magnetic Interference
ISI	Inter Symbol Interference
ROF	Radio on Fiber
UART	Universal Asynchronous Receiver Transceiver
IEEE	International Electrical and Electronic Engineer
PSK	Phase Shift Keying
FOV	Focus of Vision
OBN	Optical Beam Networking
IM	Intensity Modulation
DD	Direct Detection
CDMA	Code Division Multiple Access
WDM	Wave Division Multiplexing
LED	Light Emitting Diode
LASER	Light Amplification by Stimulating Emission of Radiation
LOS	Line of Sight
PIN	Positive Intrinsic Negative
IEC	International Electro-technical Commission
AEL	Allowable Exposure Limit
CSC	Correct Slot Choice

Chapter 1

General Introduction



1.1 General Perspective

Trends in the telecommunications and computer industries suggest that the network of the future will consist of a high capacity backbone network with short range communication links providing network access to portable communicators and portable computers. The next generation network environment will be constructed of the high-capacity backbone network and a large number of access networks. In order to realize such access networks, high speed wireless networks are required. In this vision of the future, mobile users will access to similar grade high-speed network services available to wired terminals. For this purpose, some parts of communication links need to be constructed wireless. This situation is illustrated in Fig. 1.1. During the last decade, therefore, the wireless communication technology has grown rapidly [1]–[5]. The technology base for implementing this concept does not yet exist, however. Radio technology, although well-suited for moderate-speed applications such as voice, may not be sufficient to support many high-speed applications. To illustrate the potential capacity requirements of a wireless network, consider the needs of a portable high-quality digital display. To reduce its size, weight, battery-power consumption, and cost, it may be advantageous to make it simple as possible, having little on-board computational power, and relegating intensive signal-processing tasks such as video decompression to the transmitter platform. To accomplish this, however, it will require mid-range or short-range wireless communication link switch with extremely high capacity. In an extreme case, for example, uncompressed high-definition video can require a data rate of 100 Mbit/s or more.

Moreover, radio wave transmission technology suffers from electro-magnetic interference (EMI) problems as the radio spectrum gets increasingly crowded. Now that personal communicators and wireless computer networks are evolving rapidly, the available spectrum is considered to be a scarce resource. Simultaneously, there is an increase in the interference level caused by switched power supplies and other high frequency equipment. Particularly in hospitals and industrial environments, the applicability of radio systems is

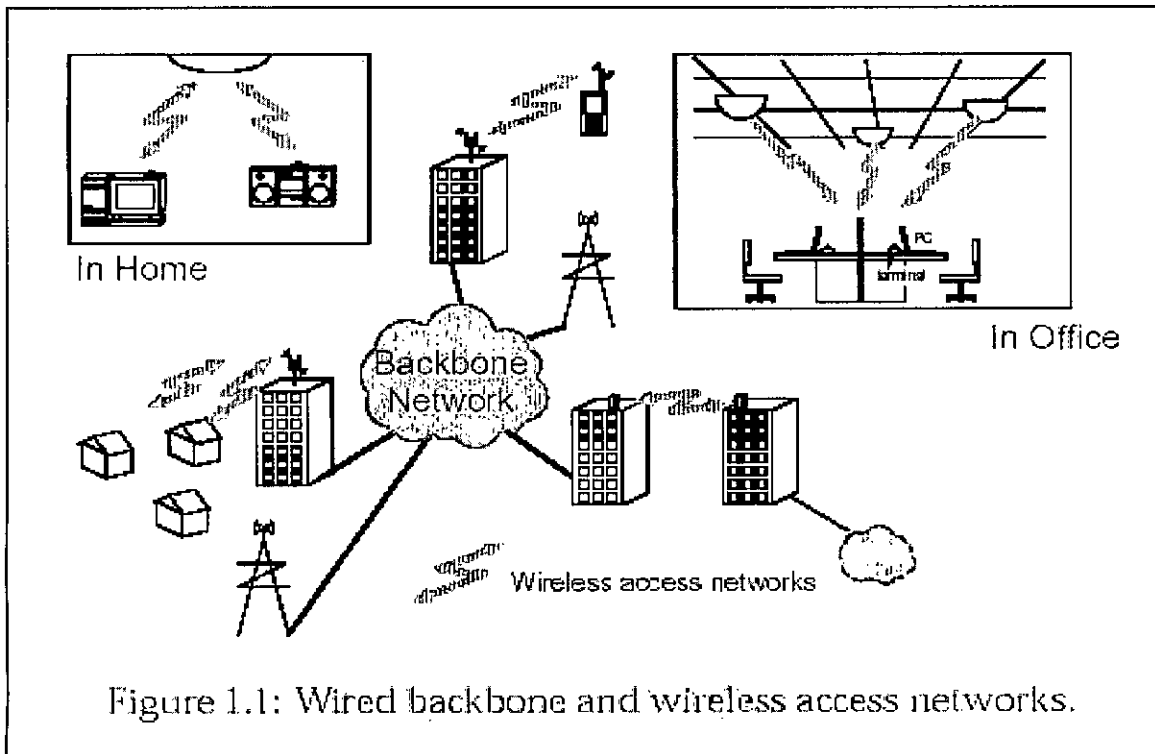
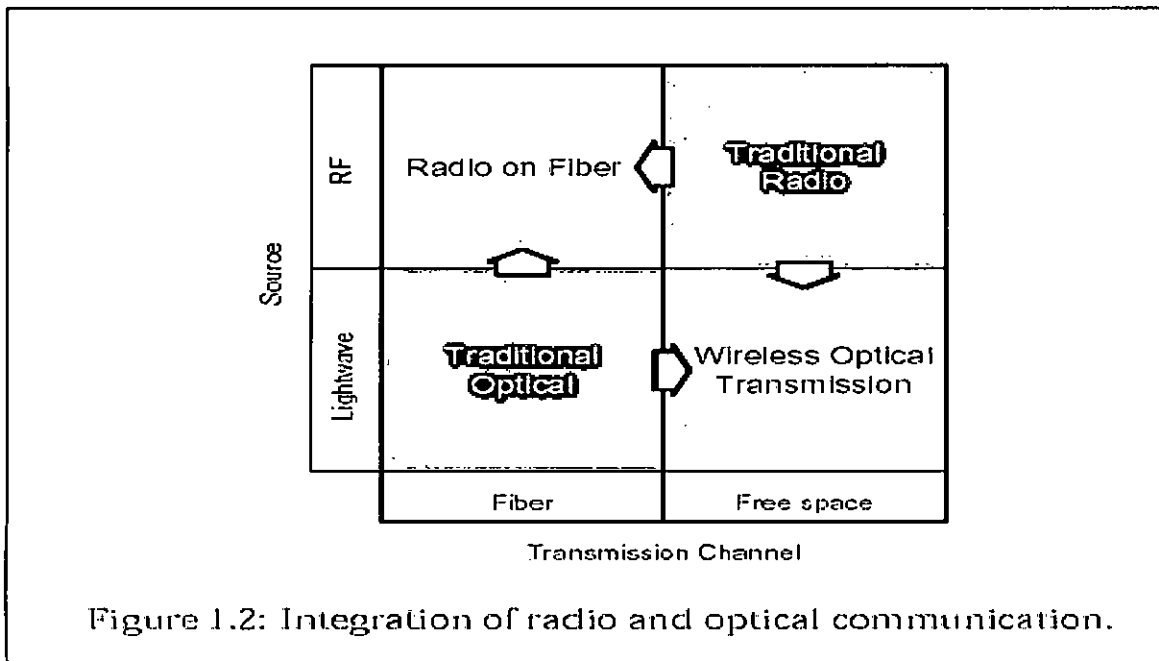


Figure 1.1: Wired backbone and wireless access networks.

already seriously limited by these problems. Extensive frequency allocation regulations can only partly solve them. Although eventually EMI aspects will become an integral part of every system design, future applications require the exploration of new wavelength ranges.

An optical wireless communication system is an attractive alternative to radio, primarily because of a virtually unlimited, unregulated bandwidth [6]–[8]. The optical spectrum is a universally available resource without frequency and wavelength regulations. An optical wireless communication system has the advantage of requiring low-cost and low power consumption components, also [9]. Moreover, for indoor applications, optical radiation is confined within a room since the radiation is either reflected or absorbed by the walls because of its short wavelength. Therefore cell planning in networks is simple and easy. In the near future, optical wireless communication system will be an attractive candidate for wireless access network.

From the view of the integration of radio and optical technology, on the other hand, an optical wireless communication technology is the important issue. Conventionally, the radio wave has been considered to be a technology for free space communication, and lightwave has been considered to be a technology for an optical fiber. Integrated technologies:



of radio and optical, however, are attracting the attention in recent years. This is illustrated in Fig. 1.2. Radio on fiber (ROF) technology is the technology for letting a radio wave pass through an optical fiber. This technology makes it possible that the data from many mobile users can be sent in an optical fiber directly. In an optical wireless communication technology, the lightwave which has been considered to be for a wired connection is emitted into the air. High capacity wireless transmission is possible in an Optical wireless technology. Thus, an optical wireless communication technology is considered to be an important technique as an integration of radio and optical technology.

1.2 Advantage of Optical Wireless communication

As a method of realizing high speed wireless networks, the optical wireless communication systems are capturing the spotlight, on the other hand. Optical wireless communication systems have the following various advantages compared with radio systems.

1. An optical carrier has wide bandwidth available, and is suitable for high speed communication networks.

2. The devices for an optical wireless transmission system are low in cost. Also no cable or fiber is needed for transmission. Thus the optical wireless communication system is suited for a consumer communication network.

3. A lightwave cannot penetrate the opaque objects such as walls. It is thought that the lightwave is secured against eavesdropping. Therefore cell planning in networks is simple and easy.

4. The optical wireless networks occupy no radio frequency spectrum and it can be used where electro-magnetic interference is strictly prohibited, such as in hospitals, airplanes, and so on.

5. The lightwaves are worldwide unregulated by any law.

Because of these features, the optical wireless communication system attracts much attention as a medium which can realize high-speed wireless networks.

1.3 Brief History of Optical Communication System

Optical communication systems date back two centuries, to the “optical telegraph” that French engineer Claude Chappe invented in the 1790’s [10]. His system was a series of semaphores mounted on towers, where human operators relayed messages from one tower to the next. It beat hand-carried messages hands down, but by the mid-19th century was replaced by the electric telegraph, leaving a scattering of “Telegraph Hills” as its most visible legacy. After passing long time, the optical fiber was invented. Optical fiber depended on the phenomenon of total internal reflection, which can confine light in a material surrounded by other materials with lower refractive index, such as glass in air. In the 20th century, inventors realized that bent quartz rods could carry light, and optical fibers went a step further. They are essentially transparent rods of glass or plastic stretched so they are long and flexible. They were used for a image-transmission by doctors in the incipient stage. The goal was to look inside inaccessible parts of the body.

On the other hand, optical transmission came to be available for the communication system after the laser as a light source was invented. As a coherent light source being not in a nature, ruby laser was invented by Dr. T. Mainman in 1960, He-Ne laser oscillated in Bel Labs next year, and GaAs semiconductor laser oscillated in 1962. The continuous oscillation of GaAlAs laser was realized in Japan, the United States and the Soviet Union in 1970, and the small semiconductor laser which could be high-speed modulated advanced optical transmission technology greatly. Around from 1965, the beam guide system which arranged the lens in a pipe, and the space propagation system which emits light to free space were beginning to be studied so as to use laser for free space optical communication. In 1979, indoor optical wireless communication system has been presented by F. R. Gfeller and U. Bapst [11]. In their system, diffuse optical radiation in the near-infrared region was utilized as signal carrier to interconnect a cluster of terminals located in the same room to a common cluster controller. However, the reduction in loss of the fiber and the invention of continuous semiconductor laser has moved the mainstream of the research to optical fiber transmission, and the utilization of optical transmission system was accelerated from 1970 to 1980.

1.4 Recent Optical Wireless Communication Systems

In the 1990s, some practical applications using optical wireless communication got actual shape, and some products and their standards were completed. Optical wireless systems are classified into two categories depending on where the system is utilized. In this section, these applications will be introduced from this point of view.

1.4.1 Indoor applications

There is a growing interest in indoor wireless networks as a consequence of the large-scale utilization of personal computers and mobile communicators. In this application, an optical wireless communication system is a candidate for the media of wireless networks. Infrared is preferred as wavelength in these applications originally. This is because essentially a large total transmission bandwidth is possible, facilitating fast transmission systems due to the very high frequency involved in optical carrier. Moreover, because of the

short wavelength, optical radiation is confined within a room since the radiation is either reflected or absorbed by the walls. Therefore cell planning in networks is simple.

IrDA links

The infrared data association (IrDA) was established in 1993 as a collaboration between major industrial organizations in order to establish an open standard for infrared (IR) data communication [12]–[17]. The resulting IrDA protocol was aimed to provide a simple, low-cost, reliable means of IR communication between devices such as portable computers, desktop computers, printers, other peripherals, and LANs using directed point-to-point connectivity. Figure 1.3 illustrates an example image of an IrDA link with which PC peripherals are connected to a PC.

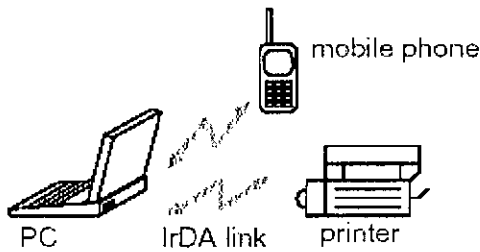


Figure 1.3: An example of an IrDA.

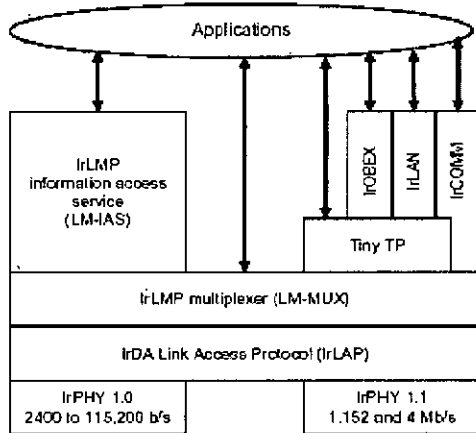


Figure 1.4: The IrDA protocol stack.

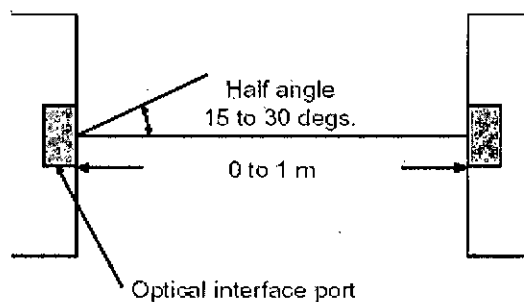


Figure 1.5: IrDA optical geometry.

IrDA links can currently provide a baud rate up to 115.2 kbit/s or 16 Mbit/s with a high-speed extension, using half-duplex point-to-point connectivity. The IrDA protocol stack is shown in Fig. 1.4. The IrDA protocol stack consists of three mandatory layers: the physical (IrPHY) layer, the IrLAP layer, and the IrDA Link Management Protocol (IrLMP) layer.

The IrDA physical layer provides half-duplex point-to-point communication through the IR medium and provides services to the upper IrLAP layer. The IR medium interface specification requires a maximum link distance of at least 1 m and a half angle range of 15 to 30 degrees. This configuration is shown in Fig. 1.5. IR transmitters have to conform to eye safety limitations on power output [18]. The maximum output intensity is specified at 500 mW/sr. Typical output power of transmitters is in tens of milliwatts range. In an IrDA link, nearly visible light (850 to 950 nm) is used. Version 1.0 of IrDA protocol stack of the physical layer provided a data rate of upto 115.2 kbit/s using a connection to the standard universal asynchronous receiver transceiver (UART) of the IrDA device.

Table 1.1: Signaling rate and pulse duration specifications of IrDA 1.4

Signaling Rate	Modulation	Pulse Duration		
		Minimum	Nominal	Maximum
2.4 kbit/s	RZI	1.41 ms	78.13 ms	88.55 ms
9.6 kbit/s	RZI	1.41 ms	19.53 ms	22.13 ms
19.2 kbit/s	RZI	1.41 ms	9.77 ms	11.07 ms
38.4 kbit/s	RZI	1.41 ms	4.88 ms	5.96 ms
57.6 kbit/s	RZI	1.41 ms	3.26 ms	4.34 ms
115.2 kbit/s	RZI	1.41 ms	1.63 ms	2.23 ms
0.576 Mbit/s	RZI	295.2 ns	434.0 ns	520.8 ns
1.152 kbit/s	RZI	147.6 ns	217.0 ns	260.4 ns
Single pulse	4PPM	115.0 ns	125.0 ns	135.0 ns
Double pulse	4PPM	240.0 ns	25.0 ns	260.0 ns
16.0 Mbit/s	HHH(1,13) ¹	38.3 ns	41.7 ns	45.0 ns

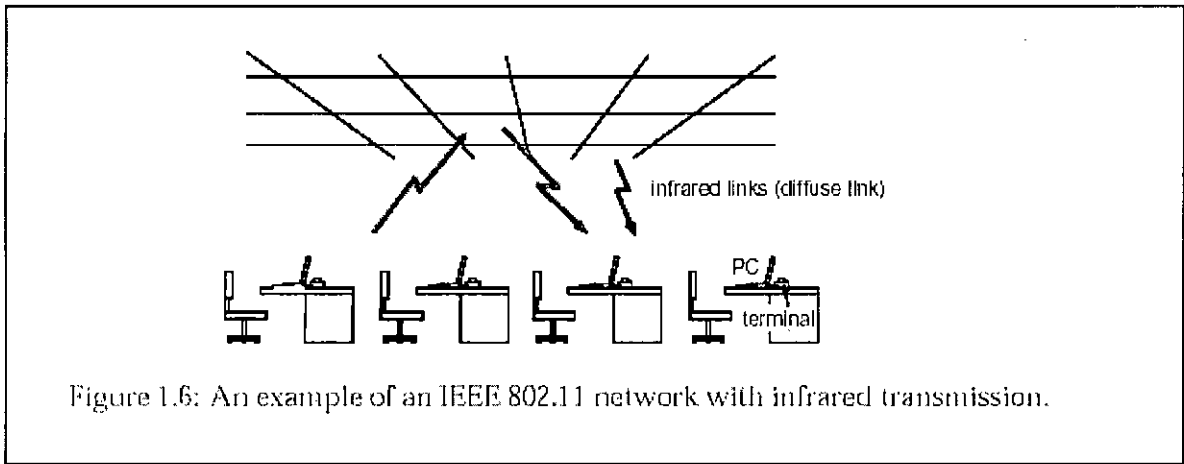
¹HHH(1,13) modulation is a newly coding which is utilized low duty cycle, rate 2/3, and (d,k) = (1,13) run-length limited(RLL)code.

The hardware typically consists of an IR transceiver module containing IR LED with output driver and IR detector and receiver, and encoding/decoding circuitry. This can be as a plug-in adapter to the portable computers. The modulation scheme is return-to-zero (RZ) with a 3/16 bit time pulse duration. Version 1.1 extends the specification to support data rates of 1.152 Mbit/s and 4 Mbit/s. The 1.152 Mbit/s system uses return-to-zero (RZ) modulation scheme as in version 1.0 of the specification, but 4 Mbit/s system requires additional hardware for a 4-pulse position modulation (PPM) scheme and phase-locked loop (PLL) detection. Version 1.4 of IrDA standard was published in 2001. This version supports data rates of 16Mbit/s with low duty cycle, rate 2/3, and $(d, k) = (1, 13)$ run-length limited (RLL) code [19]. The modulation scheme in version 1.4 is summarized in Table 1.1.

Physical layer for IEEE 802.11

IEEE 802.11 standard for wireless local area networks (Wireless LANs) defines a specification for an infrared physical layer [20], [21]. In the United States, the executive committee of the IEEE 802 project created the IEEE 802.11 group to work on the specification of a wireless LAN for different technologies, including radio and infrared. The standard was approved in June 1997. An essential characteristic of the IEEE 802.11 specification is that there is a single medium access control (MAC) sub-layer common to all physical (PHY) layers. This feature will allow easier interoperability among the many physical layers that are expected to be defined in the future, driven by the fast technological progress in this field. There are presently three different PHY layers in the standard: infrared (IR), frequency hopping spread-spectrum (FHSS), and direct sequence spread-spectrum (DSSS). Infrared and radio can be considered complementary technologies for the support of wireless LANs. Infrared technology is well suited for low-cost low-range applications, such as ad hoc networks. In these layers of the IEEE 802.11 standard, nearly visible light (850 to 950 nm) is used. Figure 1.6 illustrates an example image of an IEEE 802.11 network with infrared transmission.

The infrared PHYSICAL layer supports two data rates: 1 and 2Mbit/s. The specification of two data rates is aimed at following:



- A smooth migration to higher data rates
- Asymmetric operation of the basic service set (BSS)

A pulse position modulation (PPM) scheme is utilized in the IEEE 802.11 standard basically.

1.4.2 Outdoor applications

There are many situations where an optical fiber is not always suitable for a fixed link, example include temporary links, rapid deployment requirements and extremely cost sensitive links such as that from the curb to the house. The cost problem in the links such as that from the curb to the house is called “last one mile problem,” in particular. Radio and microwave links currently solve some of these issues, however such systems are not without some serious drawbacks, notably high cost, large physical size, the need for regulatory approval and spectrum allocation, and the low bandwidth available. Optical wireless systems can be utilized in these situations, also.

Over long distance (1 to 5 km) optical wireless solutions can offer very rapid provision of exceedingly high bandwidth at least 1 to 10 Gbit/s is easily achievable. This flexibility is brought at the price of increased downtime, due to occasionally unfavorable atmospheric conditions, but would be invaluable where bandwidth was either needed very rapidly, say for disaster recovery, or only temporarily, say at a sporting event.

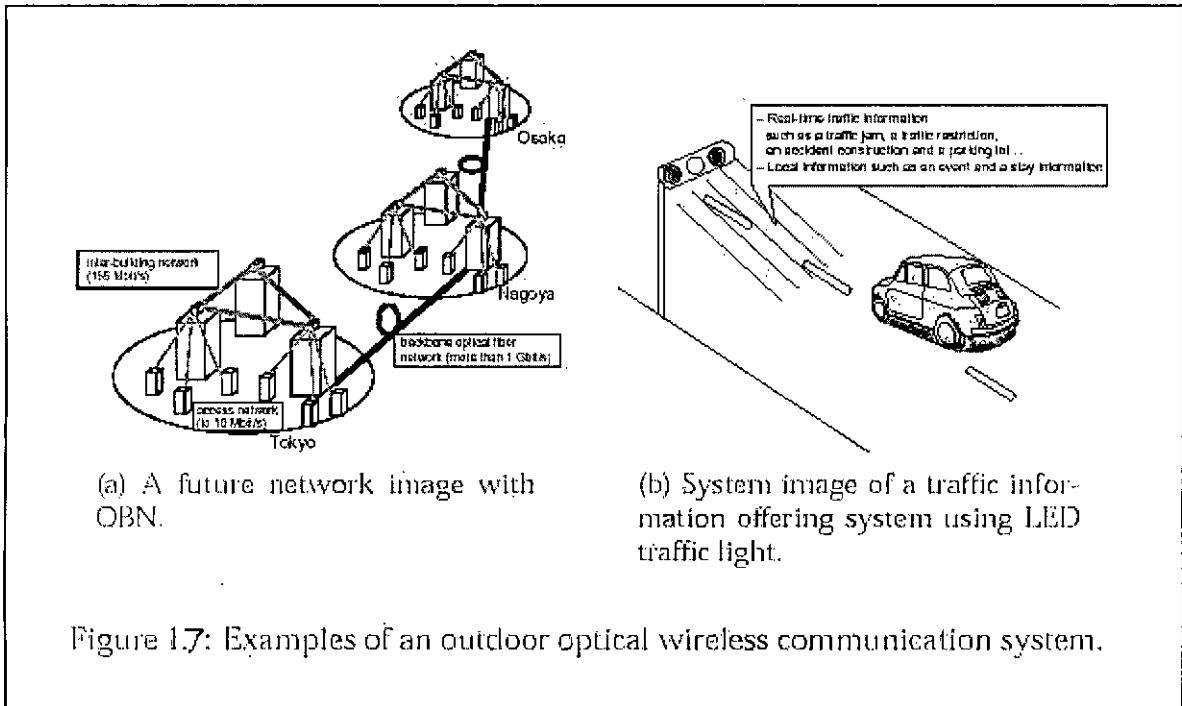


Figure 1.7: Examples of an outdoor optical wireless communication system.

Many papers concerning this advantage have been published. In [22]–[24], an inter-building optical communication system has been proposed. In these papers, an optical wireless communications system using sub carrier phase shift keying (PSK) modulation is discussed. Although this system suffers from the multiplicative intensity noise which is well-known as scintillation, 120Mbit/s data transmission was achieved. Their results were utilized for the Canobeam [25]. In the Canobeam system, 622 Mbit/s transmission with auto-tracking is available in distance between 1 to 2 km. After crude manual alignment, each end of this system locks onto the other and maintains alignment even in the event of the transmitter/receiver units being jolted or moved off axis by several degrees.

Over shorter distance, less than 500 m, permanent systems with very high availabilities can be designed. Moreover the intrinsically low cost of near infrared components, which couple into free space, can be exploited to produce a lower cost alternative to fiber for some fixed applications such as broadband signals from the curb to the home. The cost of this is dominated by two factors: the customer laser and receiver, and the cost of actually installing the fiber by digging or tunneling. This cost-problem is known as “last one mile problem.” Free space optical communication systems obviously remove the need for digging but can Also utilize cheap mass-market near infrared transmitter lasers and silicon receivers which cost at least an order of magnitude less than equivalent 1.5 μm devices fitted with single-mode

fiber. In Japan, OBN (Optical Beam Networking) council was established in 1997 so that the last one mile problem would be solved. In OBN, optical transmitters and receivers are utilized [26]. An example of a network image with OBN is shown in Fig. 1.7(a). In access networks, 10Mbit/s transmission is available, and 155 Mbit/s optical wireless transmission is available between some buildings. In [27]–[35], an information offering system with LED traffic light has been proposed. This system utilizes a traffic light comprised of LEDs, which can offer traffic information to drivers. The concept of this system is shown in Fig. 1.7(b). This information contains real-time information such as a traffic jam, a traffic restriction, an accident construction and a parking lot, or local information such as an event and a stay information. These systems are offering the information to the move objects of a car. Therefore, the wireless communication system is suitable as an access network. Moreover, the optical devices can be made from cheap cost in large quantities by using an optical wireless communication system. Some analyses in these papers show that 3.56 Mbit/s or more transmission is achieved with an LED traffic light.

1.5 Purpose and Position of This Study

Optical Wireless Communication is attracting more and more attention because of its ability to provide increased capacity, lower cost and flexibility. It becomes very popular in terrestrial application as well as in inter-satellite and satellite to ground communication [36]–[38] and also the places where fiber can't be installed very easily but large volume of data needs to be transferred. It can be used as information bridges between buildings containing cables or wireless subnet. When the atmosphere forms part of the propagating channel, scintillation, multi-scattering phenomena are recognized as being the major source of communication performance degradation, leading to link failure and system downtime.

On the other hand, OOK and PPM are the most widely used modulation technique in optical communication systems and their performance results have been compared in optical communication using an APD based receiver [39]. The performance of atmospheric optical system is strongly influenced by atmospheric molecular absorption, aerosol scattering and turbulence [40]. The performance of optical wireless communication through fog in the presence of pointing error is reported [41]. The performance of atmospheric optical system

for PPM CDMA system has also been analyzed [40]. The effect of coherence interference in optical wireless communication through multi-scattering channels has been evaluated considering an un-modulated optical carrier [42]. Much research has been published investigating multi-scattering effects using radiation transfer theory [43]-[44] and Monte-Carlo (MC) simulation tracing photon's paths [41]. The effect of backscattering-induced crosstalk in a WDM optical wireless communication system with intensity modulation and direct detection technique (IM/DD) is also recently reported [45]. However the performance results of OOK and M-ary PPM modulation techniques in optical wireless system in the presence of different types of atmospheric effects such as scintillation, multi-scattering, dispersion etc. are yet to be reported (known to the authors).

1.6 Objective of this Study

To develop an analytic approach to find the BER performance of OOK and PPM modulation in optical wireless communication system considering the effect of different types of atmospheric scattering such as scintillation, multi-scattering etc.

To evaluate the performance limitations imposed by above system impairments on OOK and M-ary PPM systems and to determine the optimum system design parameters at a given BER.

Chapter 2

Basic Knowledge for Optical Wireless Communication Systems

2.1 Comparison Between Lightwave and Radio Media

As a medium for wireless communication, lightwave radiation offers several significant advantages over radio. Lightwave emitters and detectors capable of high speed operation are available at low cost. The lightwave spectral region offers a virtually unlimited bandwidth that is unregulated worldwide. Infrared and visible light are close together in wavelength, and they exhibit qualitatively similar behavior. Both are absorbed by dark objects, diffusely reflected by light-colored objects, and directionally reflected from shiny surfaces. Both types of light penetrate through glass, but not through walls or other opaque barriers, so that optical wireless transmissions are confined to the room in which they originate. This signal confinement makes it easy to secure transmissions against casual eavesdropping, and it prevents interference between links operating in different rooms. Thus, optical wireless networks can potentially achieve a very high aggregate capacity, and their design may be simplified, since transmissions in different rooms need not be coordinated. When an optical wireless link employs intensity modulation with direct detection (IM/DD), the short carrier wavelength and large-area square-law detector lead to efficient spatial diversity that prevents multipath fading. By contrast, radio links are typically subject to large fluctuations in received signal magnitude and phase. Freedom from multipath fading greatly simplifies the design of optical wireless links.

The lightwave is not without drawbacks however. Because lightwave cannot penetrate walls, communication from one room to another requires the installation of optical wireless access points that are interconnected via a wired backbone. In many applications, there exists intense ambient light noise, arising from sunlight, incandescent lighting and fluorescent lighting, which induce noise in an optical wireless receiver. In virtually all short-range, indoor applications, IM/DD is the only practical transmission technique. The signal-to-noise ratio (SNR) of a direct detection receiver is proportional to the square of the received optical

power, implying that IM/DD links can tolerate only a comparatively limited path loss. Often optical wireless link must employ relatively high transmit power levels and operate over a relatively limited range. While the transmitter power level can usually be increased without fear of interfering with other users, transmitter power may be limited by concerns of power consumption and eye safety, particularly in portable transmitters. The characteristics of radio and indoor optical wireless links are compared in Table 2.1.

Table 2.1: Comparison between radio and IM/DD optical wireless systems

Property of Medium	Radio	IM/DD optical wireless
Bandwidth Regulated	Yes	No
Passes through wall	Yes	No
Multipath fading	Yes	No
Multipath distortion	Yes	Yes
Path loss	High	High
Dominant noise	Other users	Background light
Input $X(t)$ represents	Amplitude	Power
SNR proportional to	$\int X(t) ^2 dt$	$\int X(t) ^2 dt$
Average power proportional to	$\int X(t) ^2 dt$	$\int X(t) dt$

Radio and lightwave are complementary transmission media, and different applications favor the use of either one medium or the other. Radio is favored in applications where user mobility must be maximized or transmission through walls or over long ranges is required and may be favored when transmitter power consumption must be minimized. Lightwave is favored for short-range applications in which per-link bit rate and aggregate system capacity must be maximized, cost must be minimized, international compatibility is required, or receiver signal-processing complexity must be minimized.

2.2 Optical Wireless Link Design

Optical wireless links may employ various designs, and it is convenient to classify them according to two criteria. This classification scheme is shown in Fig. 2.1. The first criterion is the degree of directionality of the transmitter and receiver. Directed links employ directional transmitters and receivers, which must be aimed in order to establish a link, while non-directed employ wide-angle transmitters and receivers, alleviating the need for such pointing or tracking. Directed link design maximizes power efficiency, since it minimizes path loss and reception of ambient light noise. On the other hand, non-directed links may be more convenient to use, particularly for mobile terminals, since they do not require aiming of the transmitter or receiver. It is also possible to establish hybrid links, which combine transmitters and receivers having different degrees of directionality. The second classification criterion relates to whether the link relies upon the existence of an uninterrupted line of sight (LOS) path between the transmitter and receiver. LOS links rely upon such a path, which non-LOS links generally rely upon reflection of the light from the ceiling or some other diffusely reflecting surface. LOS link design maximizes power efficiency and minimizes multi-path distortion. Non-LOS link design increases link robustness and ease of use, allowing the link to operate even when barriers, such as people or cubicle partitions, stand between the transmitter and receiver. The greatest robustness and ease of use are achieved by the non-directed-non-LOS link design, which is often referred to as a diffuse link.

In a diffuse link, it is guaranteed that a single path is always present, regardless of obstacles or people impeding the LOS path. This link also allows roaming to some degree. However, the penalty of diffuse transmission is a much reduced capacity compared with an LOS link. This is entirely a consequence of the multiple signal paths reaching the receiver, which cause classic pulse spreading and inter-symbol interference. Research has shown that the theoretical capacity of a diffuse system is a function of many factors such as room size and geometry, the fabric and distribution of furnishings, and the placement and orientation of the base and user stations [11]. Generalizing, this work predicts an upper bound of about 25 Mbit/s in a room 10 m on each side, although higher rates have been demonstrated under particular conditions. Interference from ambient light is a particular issue for diffuse systems because of the extremely wide field of view of the receivers. However, the use of optical filters and robust signal formats minimizes any performance penalty that may arise. A

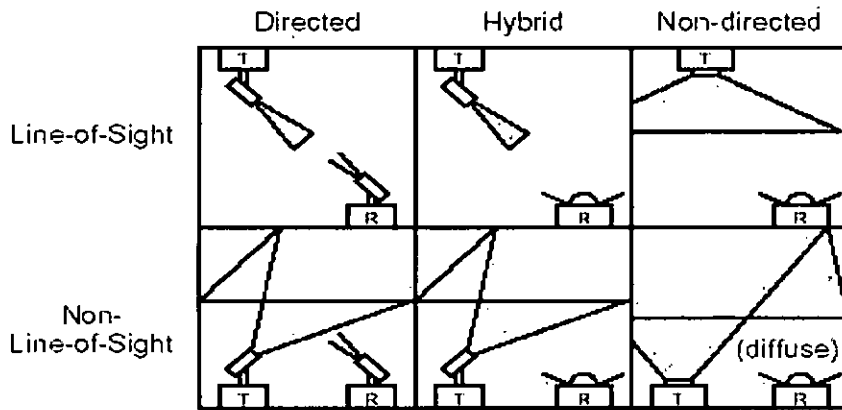


Figure 2.1: Classification of simple infrared links according to the degree of directionality of the transmitter (T) and receiver (R) and whether the link rely upon the existence of a LOS path between them

decision feedback equalizer (DFE) or maximum likelihood sequence detection (MLSD) technique can improve the performance in a diffuse link also.

2.3 IM/DD Channels

Modulation techniques for radio wireless systems include amplitude, phase and frequency modulation (AM, PM, and FM) as well as some generalizations of these techniques. Radio receivers employ one or more antennas, each followed by a heterodyne or homodyne down-converter, which is comprised of a local oscillator and a mixer. Efficient operation of this mixer relies upon the fact that it receives both the carrier and the local oscillator in a common electromagnetic mode. The down-converter output is an electrical signal whose voltage is linear in the amplitude of the received carrier electric field.

In a low-cost optical wireless system, it is extremely difficult to collect appreciable signal power in a single electromagnetic mode. This spatially incoherent reception makes it difficult to construct an efficient heterodyne or homodyne down-converter for AM, PM, and FM, or to detect AM or PM by any other means. For optical wireless links, the most viable modulation is intensity modulation (IM), in which the desired waveform is modulated onto the instantaneous power of the carrier. The most practical down-conversion technique is

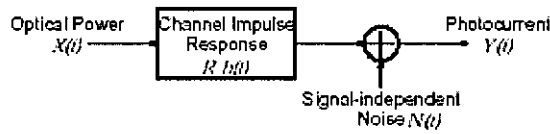


Figure 2. 2: Modeling link as a baseband filter, time-invariant system having impulse response $h(t)$, with signal-independent, additive noise $N(t)$. The photodetector has responsivity R

direct detection (DD), in which a photo detector produces a current proportional to the received instantaneous power, i.e., proportional to the square of the received electric field.

The modeling of optical wireless channels with IM/DD is illustrated in Fig.2.2. The transmitted waveform $X(t)$ is the instantaneous optical power of the lightwave emitter. The received waveform $Y(t)$ is the instantaneous current in the receiving photodetector which is proportional to the integral over the photodetector surface of the total instantaneous optical power at each location. The received electric field generally displays spatial variation of magnitude and phase, so that a multi-path fading would be experienced if the detector were smaller than a wavelength. Fortunately, typical detector areas are millions of square wavelength, leading to spatial diversity that prevents a multi-path fading. Thus when the detector is moved by a distance of the order of a wavelength, no change in the channel is observed. As the transmitted optical power $X(t)$ propagates along various paths of different lengths, optical wireless channels are still subject to multi-path distortion. This distortion is most pronounced in links utilizing non-directional transmitters and receivers, and especially when non-LOS propagation is employed. The channel can be modeled as a baseband linear system, with instantaneous input power $X(t)$, output current $Y(t)$, and an impulse response $h(t)$, as shown in Fig. 2.2. Alternately, the channel can be described in terms of the frequency response

$$H(f) = \int_{-\infty}^{\infty} h(t) e^{-j2\pi ft} dt \quad (2.1)$$

where $H(f)$ is the Fourier transform of $h(t)$. It is usually appropriate to model the channel “ $h(t) \Leftrightarrow H(f)$ ” as fixed, since it usually changes only when the transmitter, receiver or objects in the room are moved by tens of centimeters. The linear relationship between $X(t)$ and $Y(t)$

is a consequence of the fact that the received signal consists of many electromagnetic modes. By contrast, we note that when IM/DD is employed in dispersive single-mode optical fiber, the relationship between $X(t)$ and $Y(t)$ is sometimes nonlinear. In many applications, optical wireless links are operated in the presence of intense infrared and visible background light. While received background light can be minimized by optical filtering, it still adds shot noise, which is usually the limiting noise source in a well-designed receiver. Due to its high intensity, this shot noise can be modeled as additive, white, Gaussian, and independent of $X(t)$. When little or no ambient light is present, the dominant noise source is receiver pre-amplifier noise, which is also signal-independent and Gaussian (though often non-white). Thus we usually model the noise $N(t)$ as Gaussian and signal-independent. This stands in contrast to the signal-independent, Poisson noise considered in photon-counting channel models. Fluorescent lamps emit infrared that is modulated in nearly periodic fashion; when present, this adds a cyclostationary component to $N(t)$ [46], [47].

The baseband channel model is summarized by

$$Y(t) = RX(t) \otimes h(t) + N(t) \quad (2.2)$$

where the “ \otimes ” symbol denotes convolution and R is the detector responsivity (A/W). While Eq. (2.2) is simply a conventional linear filter channel with additive noise, optical wireless systems differ from conventional electrical or radio systems in several respects. Because the channel input $X(t)$ represents instantaneous optical power, the channel input is non-negative:

$$X(t) \geq 0 \quad (2.3)$$

and the average transmitted optical power P_t is given by

$$P_t = \lim_{T \rightarrow \infty} \frac{1}{2T} \int_{-T}^T X(t) dt \quad (2.4)$$

rather than the usual time-average of $|X(t)|^2$, which is appropriate when $X(t)$ represents amplitude. The average received optical power is given by

$$P = H(0)P_t \quad (2.5)$$

where the channel d.c. gain is $H(0) = \int_{-\infty}^{\infty} h(t)dt$. The performance of a wireless optical link at bit rate R_b is related to the received electrical SNR

$$SNR = \frac{R^2 P^2}{R_b N_0} = \frac{R^2 H^2(0) R_t^2}{R_b N_0} \quad (2.6)$$

assuming that $N(t)$ is dominated by a Gaussian component having double-sided power spectral density N_0 . From Eq. (2.6), we see that the SNR depends on the square of the received optical average power, implying that IM/DD optical wireless links must transmit at a relatively high power and can tolerate only a limited path loss. This stands in contrast to the case of radio wave channels, where the SNR is proportional to the first power of the received average power.

2.4 Design of Power Efficient Links

Achieving a high electrical SNR is the single biggest problem facing the designer of an optical wireless link. The difficulty arises for two reasons. Firstly, the SNR of an IM/DD link depends upon the square of the received optical average power. This implies that one should transmit at relatively high power, but available transmitter power may be limited by considerations of eye safety and power consumption. It also implies that one should design the link so as to minimize path loss and employ a receiver having a large light-collection area. Second, in many environments there exists intense ambient infrared noise, which introduces white shot noise and low-frequency cyclostationary noise into the receiver. This noise can be minimized through optical filtering and by employing a directional receiver, which can separate the desired signal from the ambient noise.

2.5 Major Components of Optical Wireless Link

An optical wireless links consists of a transmitter, wireless communication channels and a receiver as shown in Fig 2.3.

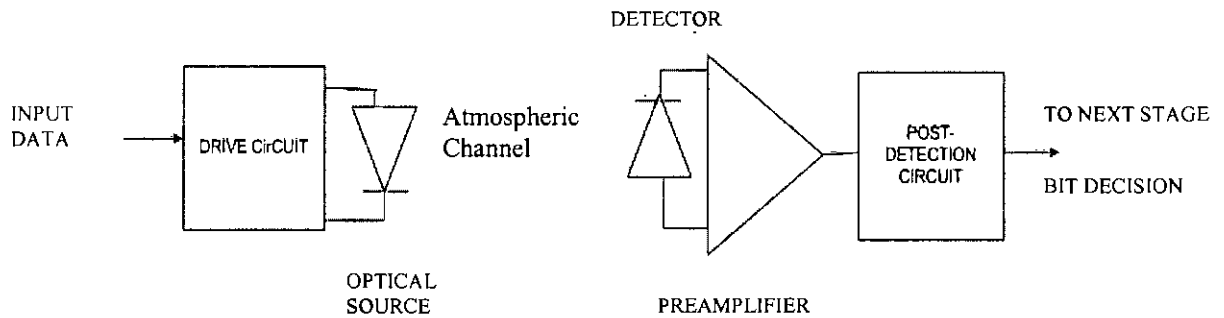


Figure 2.3: A Basic Optical Wireless Communication Link

2.5.1 Optical Sources

In most optical communication systems, semiconductor light sources are used to convert electrical signals into light. Optical sources for wireless transmission must be compatible to overcome the atmospheric effects and they should be such that one can easily modulate the light directly at high data rates. Generally either LASERS or LEDs are used in optical communication systems.

2.5.1.1 Light Emitting Diode (LED)

Light emitting diodes (LEDs) used in optical communication system are the same as visual display LEDs except that they operate in the infra-red region and with many times higher intensity of emission. When the p-n junction is forward biased, photon emission takes place due to recombination of electron-hole pair. The wavelength of emission will depend on the energy gap.

2.5.1.2 Laser

Laser stands for “light amplification by stimulating emission of radiation”. Compared to LED, a laser has wider bandwidth, higher power output, higher modulation efficiency, narrower spectral linewidth and narrower emission pattern. Laser sources are much brighter than LEDs.

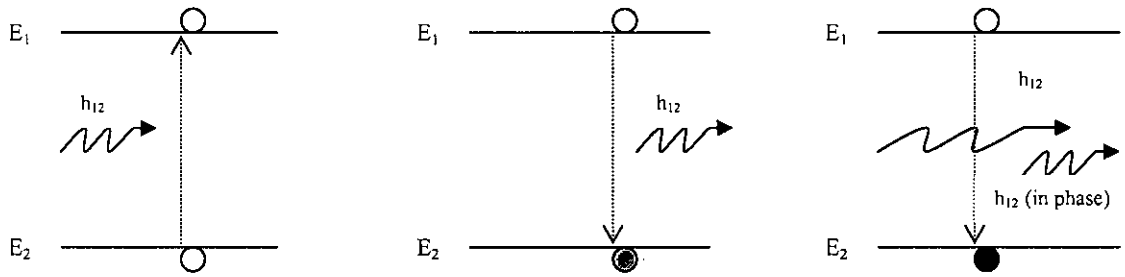


Figure 2.4: The three keys transition process involved in laser action. The open circle represents the initial state of the electron and the heavy dot represents the final state. Incident photons are shown on the left of each diagram and emitted photons are shown on the right.

Laser action is the result of three key processes [48]. These are photon absorption, spontaneous emission and stimulated emission. These three processes are represented by the simple two energy-level diagrams in Fig. 2.4, where E_1 is the ground-state energy and E_2 is the excited state energy. According to Planck's law, a transition between these two states involves the absorption or emission of a photon energy $h\nu_{12}=E_2-E_1$. Normally the system is in the ground state. When a photon of energy $h\nu_{12}$ impinges on the system, an electron in state E_1 can absorb the photon energy and be excited to state E_2 and is called absorption. Since this is an unstable state, the electron will shortly return to the ground state, thereby emitting a photon of energy $h\nu_{12}$. This occurs without any external stimulation and is called spontaneous emission. The emissions are isotropic and of random phase and, thus, appear as a narrowband Gaussian output. When a photon of energy $h\nu_{12}$ impinges on the system while the electron is in excited state, the electron is immediately stimulated to drop to the ground state and give off a photon of energy $h\nu_{12}$. This emitted photon is in phase with the incident photon and the resultant emission is known as stimulated emission.

In thermal equilibrium, the density of excited electrons is very small. Most photons incident on the system will, therefore, be absorbed, so that stimulated emission is essentially negligible. Stimulated emission will exceed absorption only if the population of the excited states is greater than that of ground state. This condition is called population inversion. Since this is not an equilibrium condition, population inversion is achieved by various "pumping" techniques. In a semiconductor laser, population inversion is accomplished by injecting electrons into the material at the device contacts to fill the lower

energy states of the conduction band. In solid-state lasers like the ruby laser or Neodymium laser, light from a powerful source is absorbed in the active medium and increases the population of a number of higher energy levels. In gas lasers a similar metastable level is preferentially populated with the help of electronic excitation.

2.5.2 Optical Detectors

An optical detector is a photon (light) to electron converter. Avalanche photo-diode (APD) and positive intrinsic negative (PIN) diode are the most commonly used detectors. The most important thing of the optical communication system is that the spectral response of both the source and the detector must be same, otherwise efficiency will suffer.

2.5.2.1 PIN diode

PIN is the simplest optical detector. It is composed of an n^+ substrate, a lightly doped intrinsic region and a thin p zone. Operated with a reverse bias, mobile carriers leave the p-n junction producing a zone of moderate electric field on both sides of the junction into the intrinsic region. As it only lightly doped, this field extends deeply. Incident light power is mainly absorbed in the intrinsic region, causing electron hole pairs to be generated. These carriers are separated by the influence of the electric field in the intrinsic region and represent a reverse diode current that can be amplified.

2.5.2.2 Avalanche Photo Diode (APD)

It is the second popular type of photodetector and has the advantage of internally multiplying the primary detected photocurrent by avalanche process, thus increasing the signal detection sensitivity. But some noises are also generated here.

The frequency response of both PIN and APD are similar, making them both suitable up to 1 GHz. The main advantage of APD over PIN diode is greater gain bandwidth product due to the inbuilt gain. Silica is the material used at short wavelength ($< 1 \mu\text{m}$), Ge, InGaAsP and AlGaAsP becoming popular at the longer wavelength around $1.3 \mu\text{m}$.

2.6 Optical Transmitters and Eye Safety

The wavelength band between approximately 780 and 950 nm is presently the best choice for most present applications of optical wireless links, due to the availability of low-cost LED's and laser diodes (LD's) and because it coincides with the peak responsivity of inexpensive, low-capacitance silicon photo diodes. The primary drawback of radiation in this band relates to eye safety i.e, it can pass through the human cornea and be focused by the lens onto the retina, where it can potentially induce thermal damage. The cornea is opaque to radiation at wavelength beyond approximately 1400 nm, considerably reducing potential ocular hazard, so that it has been suggested that the 1550-nm band may be better suited for optical wireless links. Unfortunately, the photo diodes presently available for this band, which are made of germanium or InGaAs, have much higher costs and capacitances per unit area than their silicon counterparts. To our knowledge, at present all commercially available systems operate in the shorter-wavelength band.

Table 2.2 presents a comparison between LED's and LD's. LED's are currently used in all indoor commercial systems, due to their extremely low cost and because most LED's emit light from a sufficiently large surface area that they are generally considered eye-safe. Typical packaged LED's emit light into semi-angle (at half power) ranging from approximately 10–30 degrees, making them suitable for directed transmitters. Non-directed transmitter's frequency employ multiple LED's oriented in different directions.

Table 2.2: Comparison between LED's and LD's

Characteristics	LED	LD
Spectral width	25-100 nm (10-50 THz)	$< 10^{-5}$ to 5 nm (<1 MHz to 2 THz)
Modulation Bandwidth	Tens of KHz to tens of MHz	Tens of KHz to tens of GHz
E/O Conversion Efficiency	10-20%	30-70%
Eye Safety	Generally considered eye-safe	Must be rendered eye-safe, Especially for $\lambda < 1400$ nm
Cost	Low	Moderate to high

Potential drawbacks of present LED's include:

- 1) Typically poor electro-optic power conversion efficiencies of 10–20 % (though new devices have efficiencies as high as 40 %)
- 2) Modulation bandwidths that are limited to tens of MHz in typical low cost devices²
- 3) Broad spectral widths (typically 25–100 nm), which require the use of a wide receiver optical pass band, leading to poor rejection of ambient light and
- 4) The fact that wide modulation bandwidth is usually obtained at the expense of reduced electro-optic conversion efficiency.

LD's are much more expensive than LED's, but offer many nearly ideal characteristics:

- 1) electro-optic conversion efficiencies of 30–70 %,
- 2) wide modulation bandwidths, which range from hundreds of MHz to more than 10GHz and
- 3) Very narrow spectral widths (spectral widths ranging from several nm to well below 1 nm are available).

To achieve eye safety with an LD requires that one pass the laser output through some element that destroys its spatial coherence and spreads the radiation over a sufficiently extended emission aperture and emission angle. For example, one can employ a transmissive diffuser, such as a thin plate of translucent plastic. While such diffusers can achieve efficiencies of approximately 70 %, they typically yield a Lambertian radiation pattern, offering the designer little freedom to tailor the source radiation pattern. Computer-generated holograms offer a means to generate custom-tailored radiation patterns with efficiencies approaching 100 %, but must be fabricated with care to insure that any residual image of the LD emission aperture is tolerably weak.

²Recently, RCLEDs (Resonant Cavity LEDs) have been developed. Their structures are epitaxially grown by MBE on double polished n+GaAs substrates and emit through the substrate, which is nominally transparent at these wavelengths. The active layers in the cavity are 3 or 4 strained $\text{In}_x\text{Ga}_{1-x}\text{As}$ ($x \sim 0.17$) Quantum Wells (QWs) clad by GaAs barrier layers. The bottom mirror is a multiple quarter-wave stack of GaAs/AlAs layers, known as a Distributed Bragg Reflector (DBR). The cavity is completed by the deposition of a metal mirror on the upper surface of the multilayer structure. A key property of RCLEDs of application is the ability to determine the emission angular beam profile by designing the emission wavelength of the QWs inside the cavity to be approximately 10–20 nm shorter than the resonance wavelength of the cavity. Moreover the modulation bandwidth of RCLEDs are achieved to approximately 500 MHz [49]–[51].

The eye safety of infrared transmitters is governed by International Electro-technical Commission (IEC) standards [18]. It is desirable for infrared transmitters to conform to the IEC Class 1 allowable exposure limit (AEL), implying that they are safe under all foreseen circumstances of use, and require no warning labels. At pulse repetition rates higher than 24 kHz, compliance with this AEL can be calculated on the basis of average emitted optical power alone. The AEL depends on the wavelength, diameter, and emission semiangle of the source. At present, the IEC is in the midst of revising the standards applying to infrared transmitters. Based on proposed revisions, at 875 nm, an IrDA-compliant source having an emission semiangle of 15 degrees and diameter of 1mm can emit an average power upto 28 mW. At the same wavelength, a Lambertian source (60 degrees semiangle) having a diameter of 1 mm can emit up to 280 mW; at larger diameters, the allowable power increases as the square of the diameter.

Chapter 3

Performance Analysis of OOK and M-PPM System in Direct Detection Optical Wireless Communication without Atmospheric Effects

3.1 Introduction

Direct Detection laser communication systems are potentially very promising for future deep space application, inter-satellite optical links and terrestrial line of sight communication. A direct detection receiver measures the energy in the received optical field. Signaling schemes are then limited to modulation of field intensities rather than phase or frequency and is commonly achieved by transmitting optical light pulses in some type of encoded format, viz, on-off keying (OOK), pulse position modulation (PPM), intensity level modulation etc. Among these the PPM is the most attractive modulation format for power limited space and inter-satellite optical communication links. Its use in wideband optical fibre communication is also foreseen.

The performance of direct detection OOK and PPM optical space links are well documented for shot noise limited and APD receiver. Performance degradation in the links is caused mainly by the tracking error and the shot noise process including the background optical noise from the sun and has become a serious problem. In this chapter, a theoretical analysis for direct detection laser communications receiver performance taking into account the effect of laser phase noise and receiver noise is presented. The receiver performance are evaluated and compared in terms of bit error probability versus average signal required per bit when the transmitter utilizes either on-off keying (OOK) or M-ary pulse position modulation (PPM) formats.

3.2 System Receiver Model

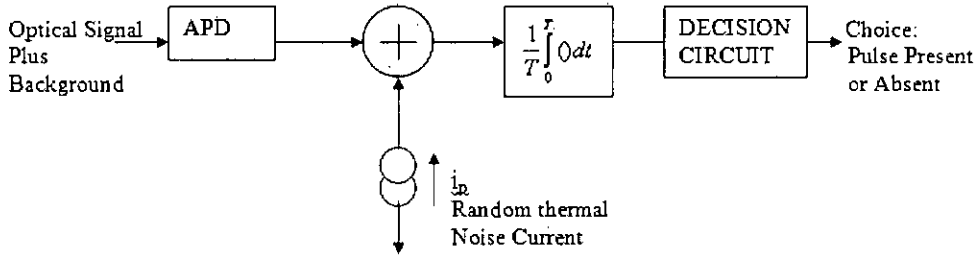


Fig. 3.1: A receiver model for optical OOK and PPM system

The model used for the optical receiver is shown in Fig.3.1. The rectangular shaped optical signal pulse corrupted by background light are detected by Avalanche Photodiode (APD) having a current gain G_{APD} , an un-amplified surface leakage current I_s and an amplified bulk leakage current I_B . Its output is summed with the random thermal noise current i_p generated by an external preamplifier and is input to a unity gain integrator such that the integrator output is proportional to the number of received signal and noise photoelectrons in the received time slot. This is sometimes called a “photon counting”. This circuit performs the operation of a maximum of posteriori (MAP) receiver for a rectangular optical input pulse. The PPM demodulator then decides which time slot is most likely to contain the pulse. The resultant stream of PPM words is converted into the original data stream by error decoder with a certain probability of bit error. For the OOK format, the integrator output is compared to a threshold and the decision circuit’s output is the receiver best estimate of the input data stream.

To simplify the calculation, the bandwidth limiting effects of APD capacitance have not been included in this model and the receiver was assumed to have a perfect clock recovery. The effects of APD capacitance are small as long as $R_L C_{APD} \ll T$. Therefore, finite C_{APD} places an upper limit on R_L . Non-ideal clock recovery causes energy spillover into

adjacent time slots that can be taken into account in the following analysis by modifying the modulation extinction ration M.

3.3 Input Signal to OOK/PPM Receiver

The optical signal input to optical receiver is

$$S(t) = \sqrt{2P_{in}} * \exp(-j(\omega_0 t + \Delta\Phi_n(t) + \theta)) \quad (3.1)$$

where P_{in} is the input optical Power, $\Phi_n(t)$ is the instantaneous phase noise of transmitting laser and ω_0 is the optical carrier frequency.

The photocurrent at the output of the photodetector is –

$$\begin{aligned} i(t) &= R_d s^2 \\ &= R_d \bar{E} [2P_{in} * \exp(-2j(\omega_0 t + \Delta\Phi_n(t) + \theta))] \end{aligned} \quad (3.2)$$

where R_d denotes the responsivity of the photodetector and E denotes Expectation.

3.4 Receiver Output Statistics

The primary photocurrent within the APD produced by the incident optical field can be accurately modeled as a Poisson point process, whose rate is proportional to the instantaneous optical intensity. This photocurrent is then randomly multiplied within the APD gain region. The probability distribution of the random APD gain has been previously derived and verified [52]. The exact formulation of the composite APD output statistics is complex and is evaluated numerically [53]. However, the APD output has been shown to be well approximated by Gaussian statistics for an optical communication receiver [54]. Therefore, the receiver performance is completely characterized by the mean and variance of the

integrated APD current conditioned on the presence or absence of the transmitted signal pulse.

If the mean signal photocount integrated over T seconds is denoted by C_s , then the mean and variance of the integrated output X when the signal is present are given by [39]

$$\langle X_s \rangle = G_{APD} \left(C_s + r_b T + \frac{I_B T}{q} \right) + \frac{I_S T}{q} \quad (3.3)$$

$$\sigma_{X_s}^2 = G_{APD}^2 F \left(C_s + r_b T + \frac{I_B T}{q} \right) + \frac{I_S T}{q} + \sigma_{th}^2 \quad (3.4)$$

where r_b is the mean background current (assumed constant), q is electron charge, I_B is APD bulk leakage current, I_S is APD surface leakage current, G_{APD} is the APD gain, F is the APD access noise factor and σ_{th}^2 is the variance of thermal noise current. In the above expression, the angle brackets denote the ensemble average.

The signal photocurrent are related to the total optical energy within the pulse by –

$$C_s = \frac{E_s \eta}{h \nu} \cos(\Delta\Phi_n) \quad (3.5)$$

where E_s is the optical Energy, $\Delta\Phi_n(t)$ random phase error due to laser phase noise, ν is the optical carrier frequency and η is the detector quantum efficiency.

The APD excess noise factor is given by

$$F = K_{eff} G_{APD} + (1 - K_{eff}) \left(2 - \frac{1}{G_{APD}} \right) \quad (3.6)$$

where K_{eff} is the effective ratio of the APD hole and electron ionization coefficients.

The variance of the integrated preamplifier noise count was derived from the variance of the preamplifier current

$$\sigma_{th}^2 = 4K_B T_r B / R_L \quad (3.7)$$

By scaling the result by q and by using the noise equivalent bandwidth of the integrator, $B=1/2T$. The result is

$$\sigma_{th}^2 = 4K_B T_r T / (q^2 R_L) \quad (3.8)$$

where the K_B is Boltzmann's constant, T_r is the receiver noise temperature and R_L is the preamplifier load resistor.

When no signal is transmitted, a small amount of signal is usually sent from the transmitter due to the device imperfections. For example, laser diode transmitters are usually biased slightly above the laser threshold to maintain stability. The modulation extinction ratio M can be defined as the ratio of intensity sent when a pulse is transmitted versus that when no pulse is transmitted. Non-ideal clock recovery also causes energy spillover into adjacent receiver channels further reducing M . Therefore the statistics when no pulse is sent are

$$\langle X_{ns} \rangle = G_{APD} \left(\frac{C_S}{M} + r_b T + \frac{I_B T}{q} \right) + \frac{I_S T}{q} \quad (3.9)$$

$$\sigma_{X_{ns}}^2 = G_{APD}^2 F \left(\frac{C_S}{M} + r_b T + \frac{I_B T}{q} \right) + \frac{I_S T}{q} + \sigma_{th}^2 \quad (3.10)$$

If the receiver preamplifier noise dominates in (3.4) and (3.10), then

$$\text{var}(X_s) = \text{var}(X_{ns}) = \sigma_{th}^2 \quad (3.11)$$

and the receiver performance is completely determined by the ratio

$$\frac{(\langle X_s \rangle - \langle X_{ns} \rangle)}{(\sigma_{th}^2)^{\frac{1}{2}}}$$

Therefore, the receiver performance depends only on the signal-to-noise ratio (SNR). However, for APD gains of 10-100 and for typical levels of preamplifier noise signal shot noise dominates in (3.4) and the above condition no longer holds. In this more typical case, all four moments of the receiver signal given in (3.3), (3.4), (3.9) and (3.10) must be used to calculate performance. These are used in the following section to compute the system performance for OOK and M-PPM modulated signaling formats.

3.5 Analysis of OOK System without Atmospheric Effects

For this format, one bit is sent and the receiver makes decision every T seconds. Here $T=1/B_r$, where B_r is the bit rate. If $\text{prob}(\text{transmit "0"}) = \text{prob}(\text{transmit "1"}) = 1/2$, then the average number of signal count required per bit is $C_s/2$. The optimum receiver threshold T_{opt} equalizes the receiver error probability for transmitted 1's and 0's which is

$$T_{\text{opt}} = (\sigma_{\text{ns}} \langle X_s \rangle + \sigma_s \langle X_{\text{ns}} \rangle) / (\sigma_s + \sigma_{\text{ns}}) \quad (3.12)$$

$$\text{where } \sigma_{\text{ns}} = [\sigma^2_{X_{\text{ns}}}]^{1/2} \text{ and } \sigma_s = [\sigma^2_{X_s}]^{1/2} \quad (3.13)$$

For best performance, T_{opt} must adapt to change in signal moments. These can be caused by fluctuations in the signal or background levels, changes in the APD gain or noise or in preamplifier noise.

The optimum receiver strategy for OOK chooses a "1" if $X > T_{\text{opt}}$, and chooses "0" otherwise. The error performance of this system is determined by the parameter

$$\begin{aligned} D_N &= \frac{\langle X_s \rangle - T_{\text{opt}}}{\sigma_s} \\ &= \frac{\langle X_s \rangle - \langle X_{\text{ns}} \rangle}{\sigma_s + \sigma_{\text{ns}}} \end{aligned} \quad (3.14)$$

which gives the "normalized distance" between the threshold and the distributed mean. Since every receiver error results in one bit error, the bit error rate probability conditioned on a given phase error $\Delta\Phi_n$ is given by:

$$\text{prob}_{\text{OOK}}(\text{bit error} / \Delta\Phi_n) = \frac{1}{2\pi} \int_{D_N}^{\infty} \exp(-x^2/2) dx \quad (3.15)$$

The unconditional bit error probability is then obtained by averaging the conditional bit error probability over the PDF of $\Delta\Phi_n$. Thus

$$P_b = \int_{-\infty}^{\infty} \text{Pr ob}(bit \text{ error} / \Delta\Phi_n) P(\Delta\Phi_n) d\Phi_n \quad (3.16)$$

where the probability density function (PDF) of $\Delta\Phi_n$ is given by

$$P(\Delta\Phi_n) = \frac{1}{\sqrt{2\pi\sigma_{\Delta\Phi_n}^2}} e^{-\frac{\Delta\Phi_n^2}{2\sigma_{\Delta\Phi_n}^2}} \quad (3.17)$$

$$\sigma_{\Delta\Phi_n}^2 = 2\pi\Delta\nu T \quad (3.18)$$

By writing the equation (3.15) simply,

$$\text{prob}_{\text{OOK}}(\text{bit error}) = \frac{1}{2\pi} \int_{D_N}^{\infty} e^{-\frac{x^2}{2}} dx$$

From which we get,

$$\text{prob}_{\text{OOK}}(\text{bit error}) = \frac{1}{2\sqrt{2\pi}} \text{erfc}\left(\frac{D_N}{\sqrt{2}}\right) \quad (3.19)$$

The detailed derivation is computed in Appendix A.

3.6 Analysis of M-PPM System without Atmospheric Effects

In this format, one signal pulse is sent per word, where each word contains $M=2^k$ time slots. Since k bits are sent per word,

Pulse Width, $T=k/(2^k B_r)$, and

Average number of signal counts per bit is C_s/k .

If the receiver makes an error and assigns the pulse to the wrong slot in a word, then the number of bit errors $\leq k = \log_2 M$. The average number of bit errors per receiver error [55] is

$$N_{BS} = (k2^{k-1})/2^k - 1 \quad (3.20)$$

which approaches $k/2$ as k gets large.

An advantage of PPM over OOK is that no adaptive threshold circuit is required. The probability of bit error for MPPM is given by

$$\text{Prob}_{M\text{-PPM}}(\text{bit error}) = N_{BS}(1 - \text{Prob}(\text{CSC}/\Delta\Phi_n)) \quad (3.21)$$

where $\text{Prob}(\text{CSC}/\Delta\Phi_n)$ denotes the probability of “correct slot choice (CSC)” conditioned on a given value of $\Delta\Phi_n$. Let X_s denote the photocount (integrator) output of the pulsed slot and X_{ns} denote the photocount output of an arbitrary noise slot.

Then the probability that the noise output is less than the signal output is given by

$$P(X_{ns} < X_s) = \int_{-\infty}^{X_s} P_{X_{ns}}(X_{ns}) dX_{ns} \quad (3.22)$$

If the transmitter sent the pulse in the i^{th} time slot, then

$$\text{Prob}(\text{CSC}/\Delta\Phi_n) = \text{Prob}(X_i > X_j, \text{ for all } j \neq i) \quad (3.23)$$

Since X has a Gaussian statistics, the conditional probability of correct slot choice is

$$\text{Prob}(\text{CSC}/\Delta\Phi_n) = \int_{-\infty}^{\infty} P_{X_s}(X_s) \left[\int_{-\infty}^{X_s} P_{X_{ns}}(X_{ns}) dX_{ns} \right]^{M-1} dX_s \quad (3.24)$$

where the receiver probability densities P_{X_s} and $P_{X_{ns}}$ are normal with means $\langle X_s \rangle$ and $\langle X_{ns} \rangle$ and variances $\sigma_{X_s}^2$ and $\sigma_{X_{ns}}^2$ respectively.

The unconditional probability of correct slot choice is then obtained as

$$\text{Prob}(\text{CSC}) = \int_{-\infty}^{\infty} \text{Prob}(\text{CSC}/\Delta\Phi_n) P(\Delta\Phi_n) d(\Delta\Phi_n) \quad (3.25)$$

The unconditional bit error probability is then given by

$$\text{Prob}_{\text{M-PPM}}(\text{bit error}) = N_{\text{BS}}(1 - \text{Prob}(\text{CSC})) \quad (3.26)$$

The simplification form of equation (3.26) for computer program is derived in Appendix B.

Hermite Polynomial has been used for evaluating the integration of the equation which is depicted in Appendix C.

Chapter 4

Performance Analysis of OOK and M-PPM system in Direct Detection Optical Wireless Communication in the Presence of Atmospheric Effects

4.1 Introduction

Optical wireless communication has been the subject of much research in recent years because of the increasing interest in laser satellite-ground links and urban optical wireless communication. The major sources of performance degradation have been identified as the atmospheric scintillation, coherence interference due to multiscattering, dispersion etc. resulting in reduced power reception, intersignal interference as well as noise due to receiver circuitry and background illumination. In this chapter we will evaluate the performance of OOK and M-PPM signal in an optical wireless communication system in the presence of atmospheric scintillation as well as multiscattering channel.

4.2 Performance Analysis with Atmospheric Scintillation

In the atmospheric optical communication systems using intensity-modulation and direct-detection (IM/DD) the primary factor affecting the performance of the systems is intensity fluctuation that is known as the log-normal intensity scintillation. The atmospheric propagation path is characterized by molecular absorption aerosol scattering and turbulence [56] [57]. In clear weather, the molecular constituents of the atmosphere give rise to a variety of absorption bands.

The atmospheric propagation loss for an L long path is $\exp(-\beta L)$, where β is the extinction coefficient [23]. At visible wavelengths, the relation can be approximately modeled as $\exp(-V\beta) = 0.01$, where V km is the visibility [23]. Visibility measurement can thus be used to estimate the attenuation of optical power through atmosphere. Line of sight (LOS) laser beam propagation through the atmosphere is subject to the following undesirable effects: absorption-induced attenuation, depolarization, beam spread, angular spread, multipath spread and time-dependent fading (Doppler spread). In an M-PPM direct-detection system, depolarization is irrelevant. Assuming same for the OOK, turbulence-induced multipath spread is sub picoseconds, and hence negligible for the data rates of a few hundred mbps. We assume that the transmitter-beam divergences and the receiver field of view cone angle both exceed 1 mR. Thus the beam spread and the angular spread can be neglected. Under these conditions, only attenuation and scintillation need to be considered. For IM/DD systems, the received optical power P can be written as [40]:

$$P = \alpha P_s \quad (4.1)$$

where P_s is the received optical power without scintillation, α is the scintillation characterized by the stationary probability process and its probability density function $\rho(\alpha)$ can be written as [23]

$$\rho(\alpha) = \frac{1}{2\pi\sigma_s^2\alpha} \exp\left\{-\left(\ln\alpha + \frac{\sigma_s^2}{2}\right)/2\sigma_s^2\right\} \quad (4.2)$$

where the average of scintillation α is normalized to unity and σ_s^2 is logarithm variance of α and defined as Scintillation index. The variance $\sigma_s^2 \ll 1$ determined by the atmosphere state.

Using the receiver model mentioned earlier, at a given value of scintillation parameter the mean signal photocurrent integrated over T seconds can be written as

$$C = \alpha C_s \quad (4.3)$$

Then the mean and variance of the integrated output X when the signal is present can be written as

$$\langle X_s \rangle = G_{APD} \left(\alpha C_S + r_b T + \frac{I_B T}{q} \right) + \frac{I_S T}{q} \quad (4.4)$$

$$\sigma_{X_s}^2 = G_{APD}^2 F \left(\alpha C_S + r_b T + \frac{I_B T}{q} \right) + \frac{I_S T}{q} + \sigma_{th}^2 \quad (4.5)$$

and when no signal is present :

$$\langle X_{ns} \rangle = G_{APD} \left(\frac{\alpha C_S}{M} + r_b T + \frac{I_B T}{q} \right) + \frac{I_S T}{q} \quad (4.6)$$

$$\sigma_{X_{ns}}^2 = G_{APD}^2 F \left(\frac{\alpha C_S}{M} + r_b T + \frac{I_B T}{q} \right) + \frac{I_S T}{q} + \sigma_{th}^2 \quad (4.7)$$

Now the probability of BER can be determined as a function of α . As the scintillation is different at different position of atmosphere and is characterized by the stationary probability process, so if the probability of BER for a given α be BER_α , then the overall BER can be determined by:

$$BER = \int_0^1 (BER_\alpha) \rho(\alpha) dX \quad (4.8)$$

So, the BER for the OOK signal considering scintillation can be represented by

$$(BER)_{OOK} = \int_0^1 (BER_\alpha)_{OOK} \rho(\alpha) dX \quad (4.9)$$

and for the M-PPM signal :

$$(BER)_{M-PPM} = \int_0^1 (BER_\alpha)_{M-PPM} \rho(\alpha) dX \quad (4.10)$$

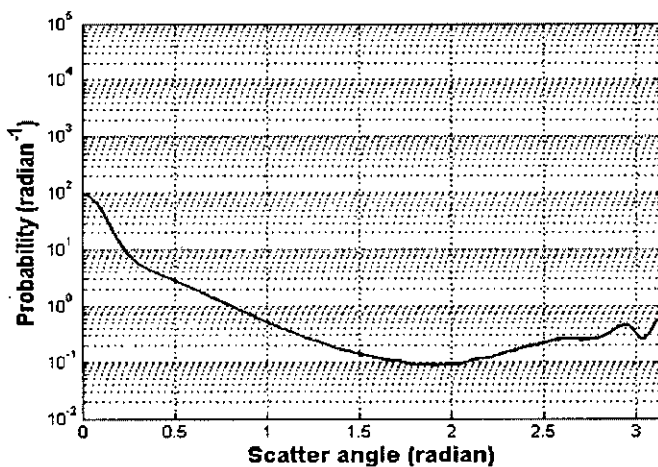
4.3 Performance Analysis with Atmospheric Scintillation and Multiscattering

In the arena of optical wireless communication, if the propagating channel is a scattering medium such as fog or a haze, then the light arriving at the receiver will no longer display the coherence properties that would have been evident had the channel in free-space. The light reaching the receiver will comprise a superposition of scattered and un-scattered waves of same frequency. The scattered waves will arrive with different phases relative to the un-scattered light due to different optical paths, they have traversed and will have amplitudes determined by the scattering cross-section of the scattering particles.

The scattering of waves by a random distribution of isotropic particles has been treated by many researchers [58] [59]. The precise scattering mechanism of light propagating in a medium is dependent on the ratio of the particle radius and the radiation wavelength. When the scattering particles are of the order of magnitude of the radiation wavelength, as is the case for optical wireless communication through fogs and hazes at visible and near-infrared wavelengths, Mie scattering is operative. Since it is the ratio of the particle radius and the wavelength that determines the scatter regime, a specific wavelength will be transmitted differently as the fog profile changes. The deflection angle of the scattered wave is described by the normalized Mie phase function, which is the probability distribution of the scatter angle. In our work, we have used the widely accepted probability distribution of the scatter angle for medium and heavy fog model (Fig. 4.1) based on extensive measured data [60]-[62] in an attempt to explore the phenomenon of coherence interference in optical wireless communication through different multi-scattering channels and to evaluate the influence on the BER performance. The two fogs, described henceforth as heavy and moderate, are distinguished both by average free path between particles and by the particle size distribution. These two parameters determine the optical density (OD) of the medium for a given propagation distance. Since the OD determines the operability of a communication link, the maximum transmission range is limited by the nature of the fog.

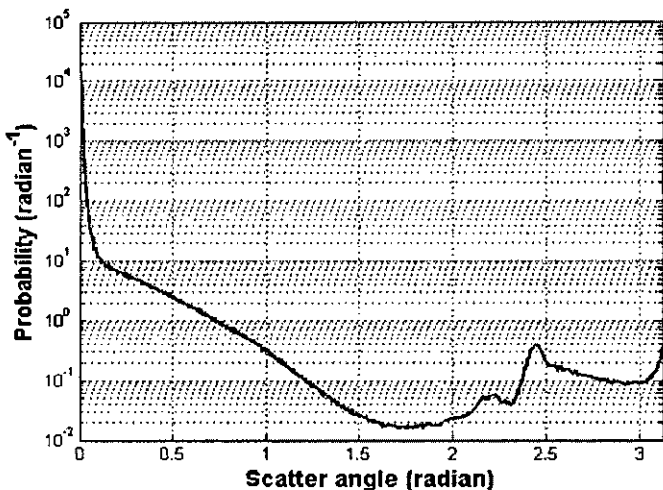
The amplitude of an un-scattered wave decreases at a rate determined by the extinction coefficient of the medium, due to absorption and scattering. In this work, absorption contribution to signal attenuation is not considered which is low at the wavelength

investigated (670 nm). The OD is the product of extinction coefficient and the transmission range. Hence, for a given OD value, the unscattered wave will be of the same amplitude regardless of the nature of the fog, and despite the difference in actual transmission range.



(a)

Probability distribution functions of scatter angle for (a) moderate fog



(b)

(b) heavy fog derived using Mie theory

Figure 4.1: Probability distribution functions of scatter angle

In contrast, the relative amplitude of the scattered wave by comparison with the wave incident on the particle is determined by the scattering particle's size, shape, and material properties (refractive index) and is summed up in the scattering cross-section. The actual amplitude of the scattered wave is hence also dependent on the position of the scattering particle and will be larger the greater the proximity of the particle to the transmitter when the un-scattered wave has not yet been severely attenuated. However, the scattered wave is attenuated in the same way as the un-scattered wave as it progresses through the propagation channel, so that, as a first approximation, we will assume that the amplitude of a single-scattered wave at the receiver is not dependent on the location of the scattering particle. This is reasonable in view of the fact that the received light arrives within a narrow angular range determined by the receiver field of view (FOV) so that the increase in the optical paths traversed by the scattered light will not be large relative to the direct line-of-sight (LOS) optical path. In addition, we will assume an average size and a spherical shape for the scattering particles for the computation of the scattered wave which will lead to the fact that the amplitude of each scattered wave will be identical.

At the receiver, un-scattered modulated light from the transmitter mixes with the scattered fields reaching the receiver after single or multiple scattering. The un-scattered light arriving at the receiver is described by $E \cos \omega t$, where E is the field amplitude and ω is the laser central wavelength. Let ϵ_i is the amplitude of the i^{th} received scattered field and ϕ_i is its phase delay. We assume that the receiver FOV is sufficiently narrow that the angle of arrival of the scattered field's wave fronts is very close to the LOS direction of arrival of the un-scattered light, and the total received field is given by the sum of the two terms:

$$E_{tot} = E \cos \omega t + \sum_{i=1}^N \epsilon_i \cos(\omega t + \Phi_i) \quad (4.11)$$

The time-averaged optic power is given by [42]

$$P(\Phi) = \frac{E^2}{2} + \frac{\epsilon^2}{2} + E \sum_{i=1}^N \epsilon_i \cos(\Phi_i) + (1/2) \sum_{i=1}^N \sum_{j=1, j \neq i}^N \epsilon_i \epsilon_j \cos(\Phi_i - \Phi_j) \quad (4.12)$$

where the complex degree of coherence is assumed to be unity. The derivation of the distribution of φ_i using the scattering medium's impulse response is described in Ref [63]. The first two terms on the right hand side of the above equation are the time-averaged intensities of the un-scattered and scattered waves alone. The second two terms represent wave phenomena of signal mixing and are not evident in the analytic approach using particle model for light. The first of the mixing term represents the mixing of the un-scattered field with the scattered fields and the second term represent the intermixing of the scattered field with one another which is not considered for this analysis to make it easier and the fact that as they are different in phase and also very small.

Considering of all the possible permutations of phase angles for the scattered waves generates the probability functions of the phase lag of the scattered waves relative to the un-scattered wave. Hence, the total received intensity, as a function of the phase lag Φ , can be found from the product of the intensity $P(\Phi)$ and the probability function of the phase delay $f(\Phi)$. The average intensity is thus given by

$$P_{av} = \frac{1}{2\pi} \int_0^{2\pi} P(\Phi) f(\Phi) d\Phi \quad (4.13)$$

The variance of $P(\Phi)$ represents the optic power due to coherence interference and is given by

$$\sigma_{co-int}^2 = \frac{1}{2\pi} \int_0^{2\pi} [P(\Phi) - P_{av}]^2 f(\Phi) d\Phi \quad (4.14)$$

This coherence power will be introduced in the received optical power for OOK and M-PPM modulated signal in optical wireless communication through multi-scattering channel when the signal will be present. Scaling the σ_{co-int}^2 by q^2 , the variance of the integrated output X when signal is present is given by

$$\sigma_{X_s}^2 = G_{APD}^2 F(\alpha C_s + \eta_b T + I_B T / q) + I_S T / q + \sigma_{ip}^2 + \sigma_{co-int}^2 T^2 / q^2 \quad (4.15)$$

Then using this σ_X^2 , the BER rate for OOK and M-PPM system considering atmospheric scintillation as well as multiscattering channel can be obtained as

$$(BER)_{OOK} = \int_0^1 (BER_\alpha)_{OOK} \rho(\alpha) dX$$

$$(BER)_{M-PPM} = \int_0^1 (BER_\alpha)_{M-PPM} \rho(\alpha) dX$$

Chapter 5

Results and Discussion

5.1 Introduction

The simulation results are presented and discussed in this chapter. The bit error rate (BER) performance, sensitivities and penalties are calculated as functions of the relevant receiver and atmospheric parameter for direct detection OOK and MPPM schemes. Also the performance comparisons between the two different schemes have been presented in details.

5.2 Results and Discussion

In order to determine the effect of atmospheric scintillation and multiscattering channel on the performance of OOK and direct detection M-ary PPM schemes, it has been evaluated numerically the bit error rate (BER) performance as a function of average signal count per bit considering the effect of shot noise, thermal noise, spontaneous emission noise and laser phase noise. The nominal values of the parameters which are used through the calculation are given in Table 5.1.

First the bit error rate performance have been calculated for different value of average signal count per bit with APD gain, wavelength and optical bandwidth as a parameter and plotted against average signal count per bit. Then the effect of atmospheric scintillation is considered and the BER performance is evaluated . Finally multiscattering effect is considered and the BER performance is evaluated for a fixed value of scintillation. From the family of performance curves, the receiver sensitivity has been calculated for a bit error rate of 10^{-9} .

Table 5.1: Nominal Parameters of Optical Wireless Communication link

Parameter Name	Value
Bit Rate, B_r	1 Gbps
Wavelength, λ	670 nm
APD Gain, G_{APD}	250
Load Register, R	200
Receiver Noise Temperature, T_r	
Surface Leakage Current, I_s	10e-9
Bulk Leakage Current, I_B	0.1e-9
Detector Quantum Efficiency, η	0.9
Effective ratio of the APD hole and electron ionization coefficients, K_e	0.02

Fig. 5.1 shows the bit error rate performance of direct detection OOK and M-ary PPM receiver without considering any atmospheric affects. The plot of BER as a function of average photon count per bit in the presence of atmospheric scintillation is depicted in Fig. 5.2 and Fig. 5.3 for OOK and M-ary PPM ($M=2,4,8$) modulation with scintillation variation (σ_s^2) as a parameter. It is noticed that there is a significant amount of degradation in receiver sensitivity due to the effect of atmospheric scintillation which is compared Fig. 5.7. Similar plots for higher value of scintillation variation (σ_s^2) are presented in Fig. 5.4, 5.5, 5.6 and they are compared in Fig. 5.8. A comparison of the results show that the effect of scintillation is much more prominent in the case of BPPM ($M=2$) and OOK and minimum in the case of OPPM system ($M=8$) due to higher energy efficiency of higher order PPM systems. For example, the receiver sensitivity in average signal count per bit corresponding to $BER=10^{-9}$ are found to be 120.7, 175.9, 206 and 336.3 for OPPM, QPPM, OOK and BPPM respectively at a bit rate of 1 Gbps with scintillation variance of $\sigma_s^2=0.01$. The corresponding receiver sensitivities are much higher at higher values of σ_s^2 . The penalty suffered by the system due to atmospheric scintillation at a BER of 10^{-9} is depicted in Fig. 5.9 as a function of scintillation variance, σ_s^2 . It is found that the penalty is significantly higher at higher values of σ_s^2 . For example, the penalty in terms of average photon count per bit is found to be 25.65, 38.5, 42.2 and 67.2 for OPPM, QPPM, OOK and BPPM respectively corresponding to $\sigma_s^2=0.005$. The penalty values are 85.55, 124.4, 133.4 and 227.6 for $\sigma_s^2=0.05$. It is thus noticed

that OPPM suffers least amount of performance degradation compared to other modulation formats.

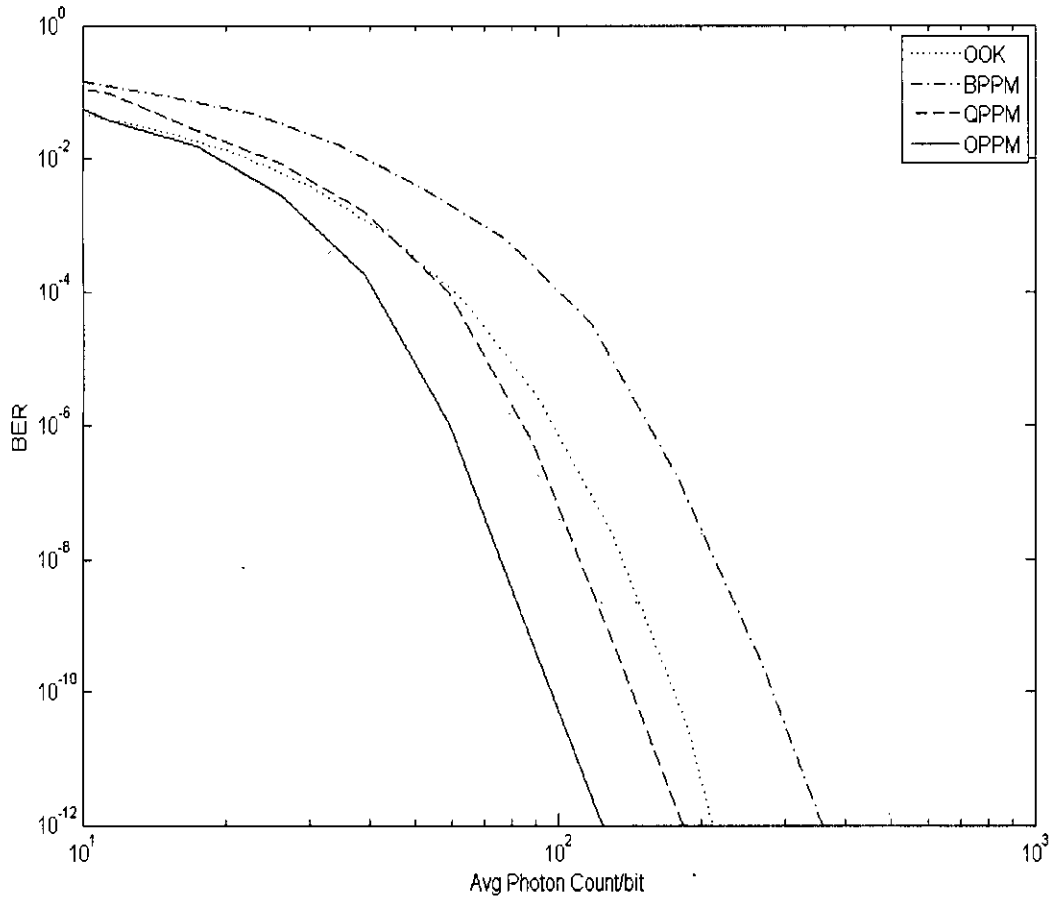


Fig. 5.1: Performance of optical OOK and M-PPM receiver without atmospheric effects

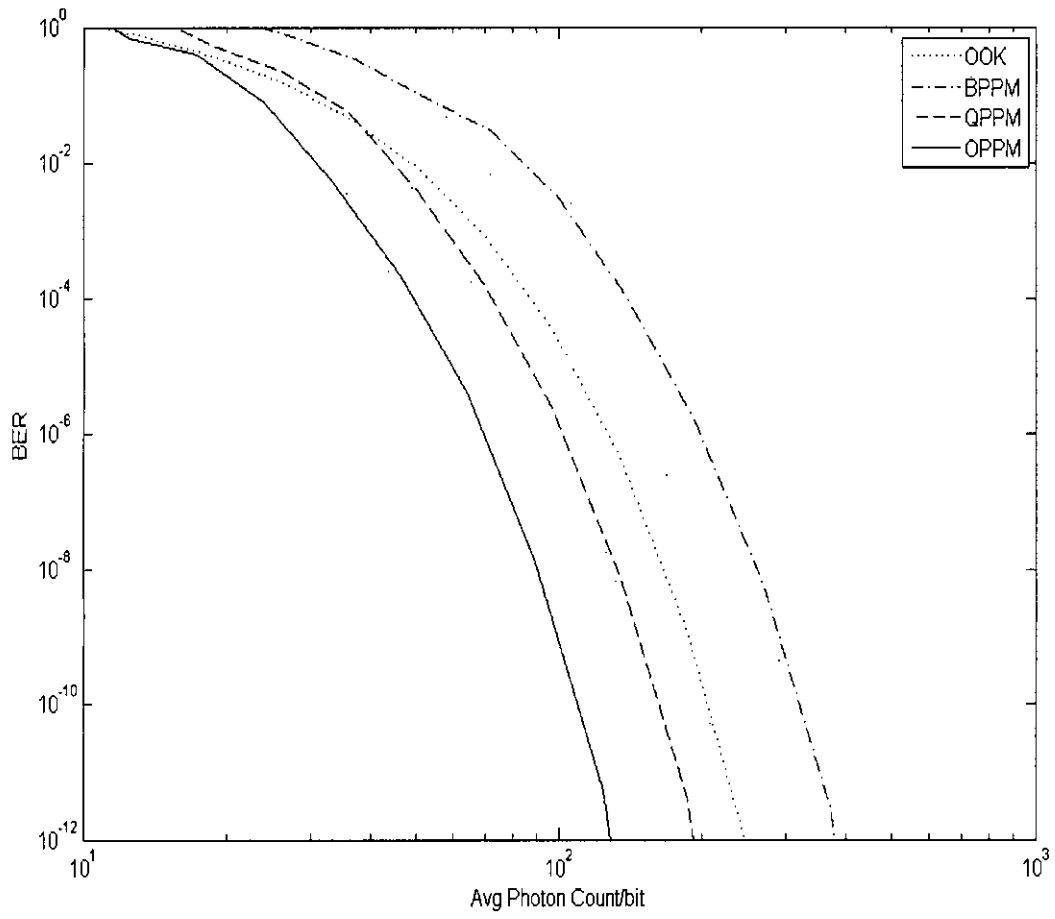


Fig. 5.2: Performance of optical OOK and M-PPM receiver in the presence of atmospheric scintillation ($\sigma_s^2=0.001$)

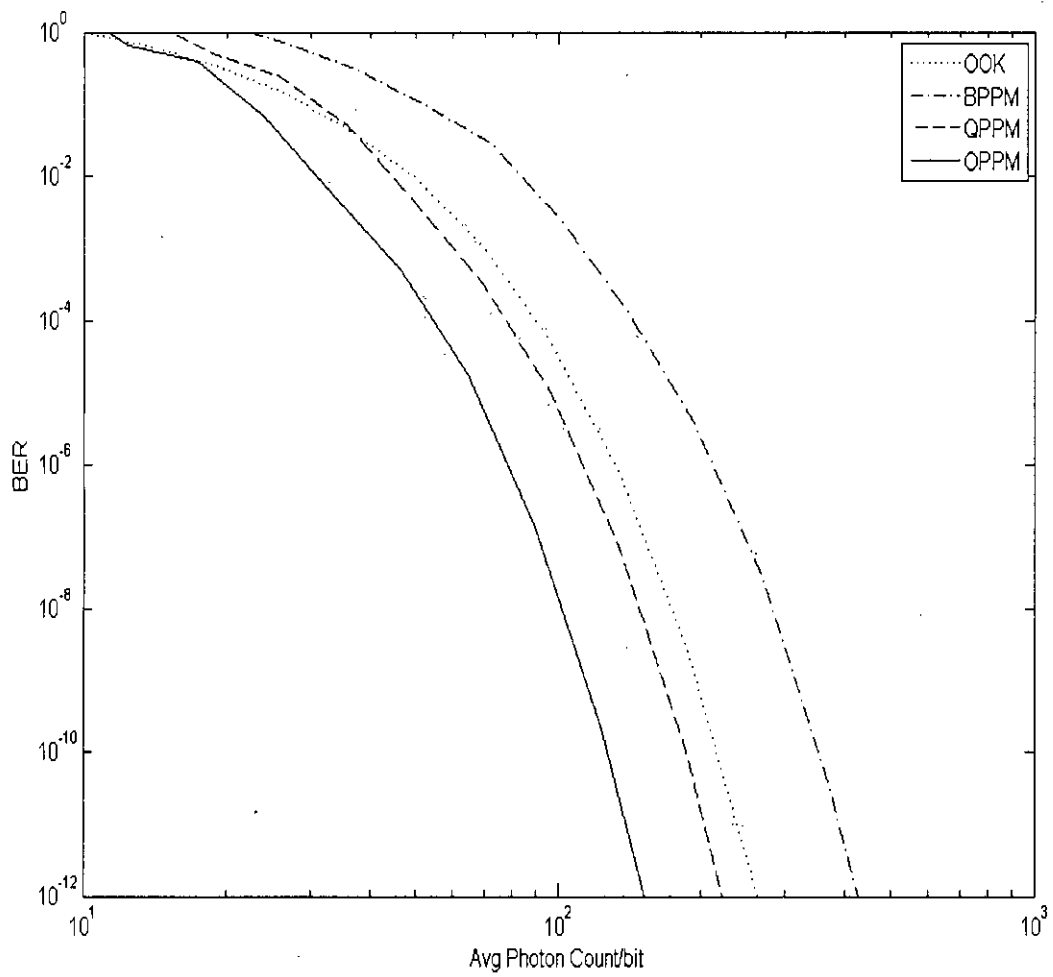


Fig. 5.3: Performance of optical OOK and M-PPM receiver in the presence of atmospheric scintillation ($\sigma_s^2=0.005$)

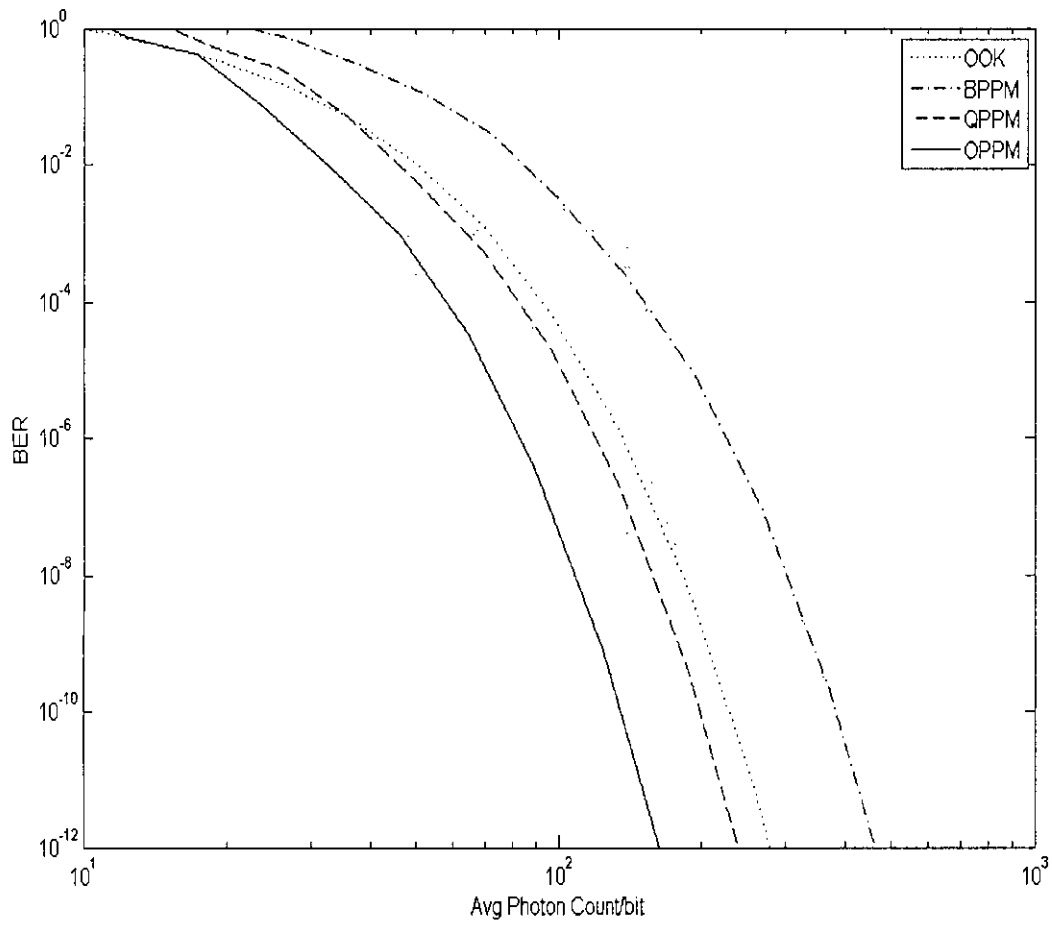


Fig. 5.4: Performance of optical OOK and M-PPM receiver in the presence of atmospheric scintillation ($\sigma_s^2=0.01$)

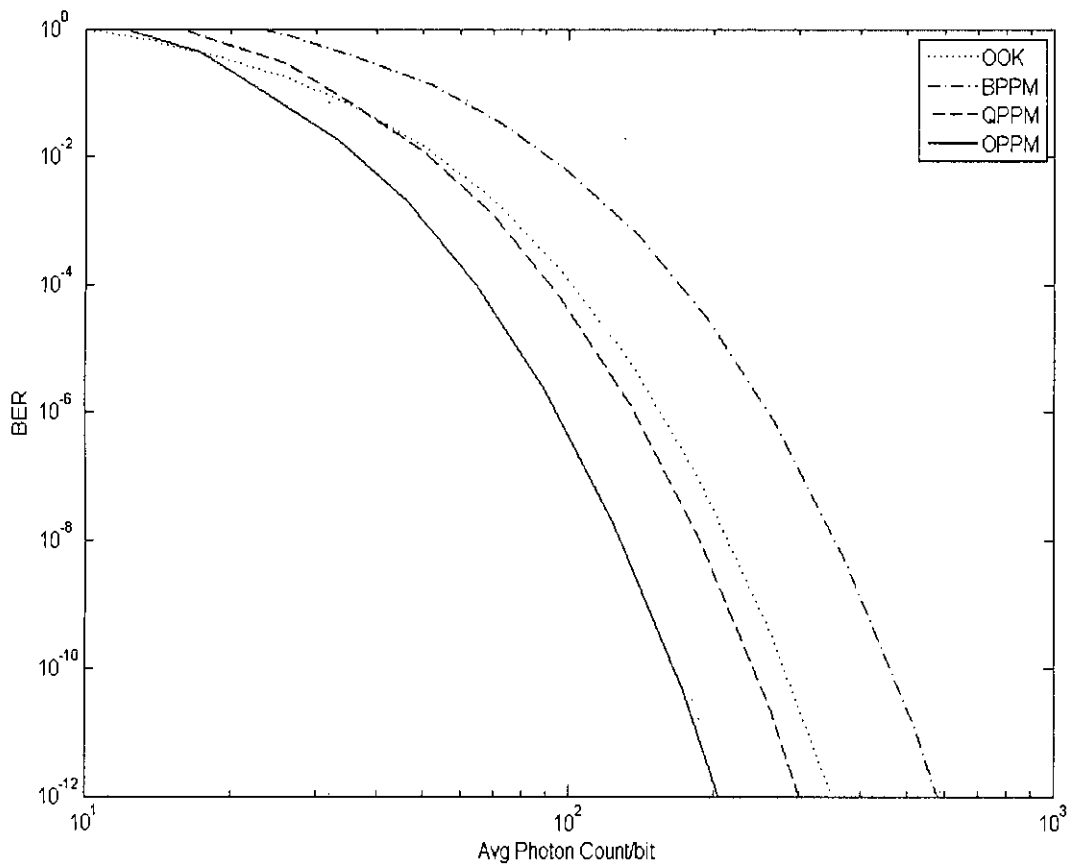


Fig. 5.5: Performance of optical OOK and M-PPM receiver in the presence of atmospheric scintillation ($\sigma_s^2=0.03$)

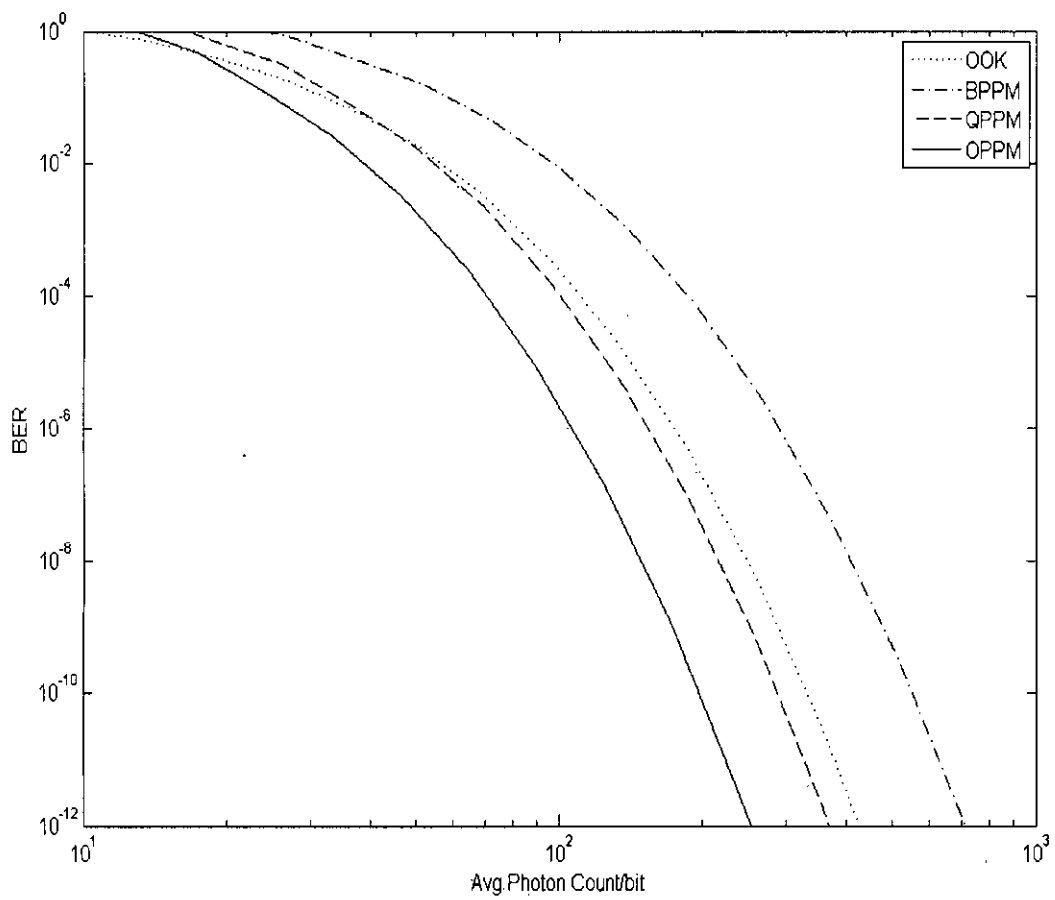


Fig. 5.6: Performance of optical OOK and M-PPM receiver in the presence of atmospheric scintillation ($\sigma_s^2=0.05$)

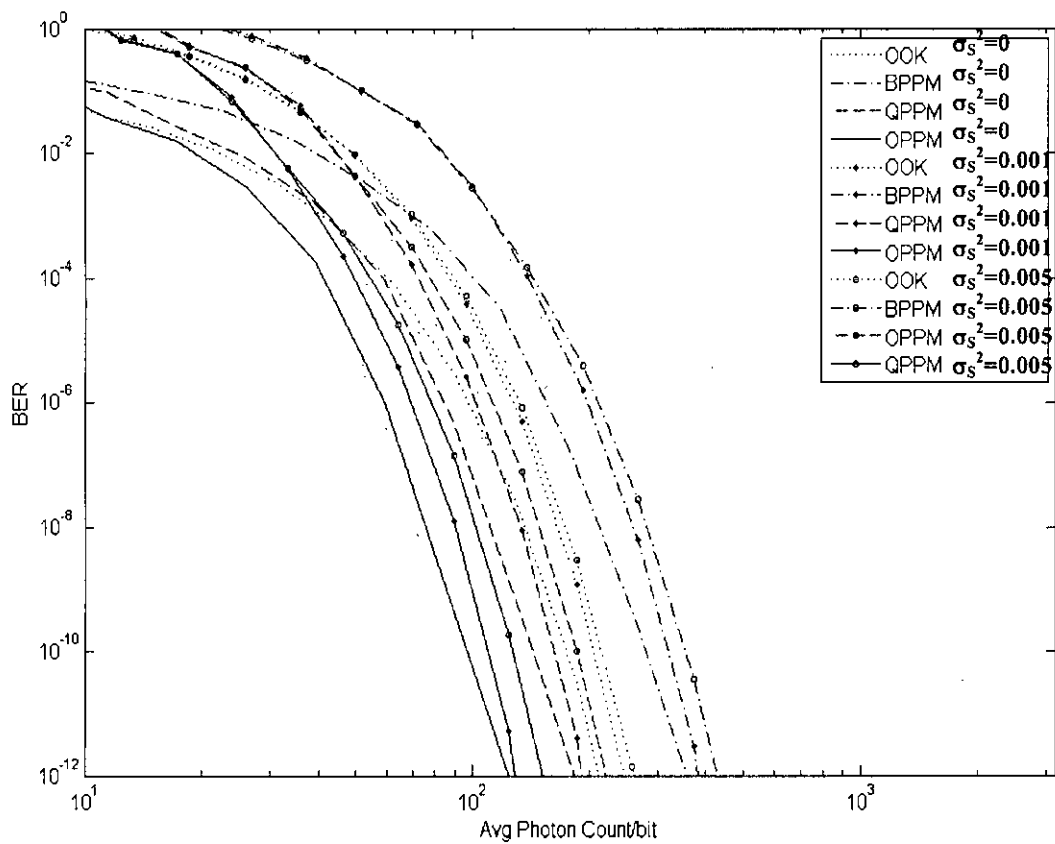


Fig. 5.7: Performance of optical OOK and M-PPM receiver in the presence of lower atmospheric scintillation

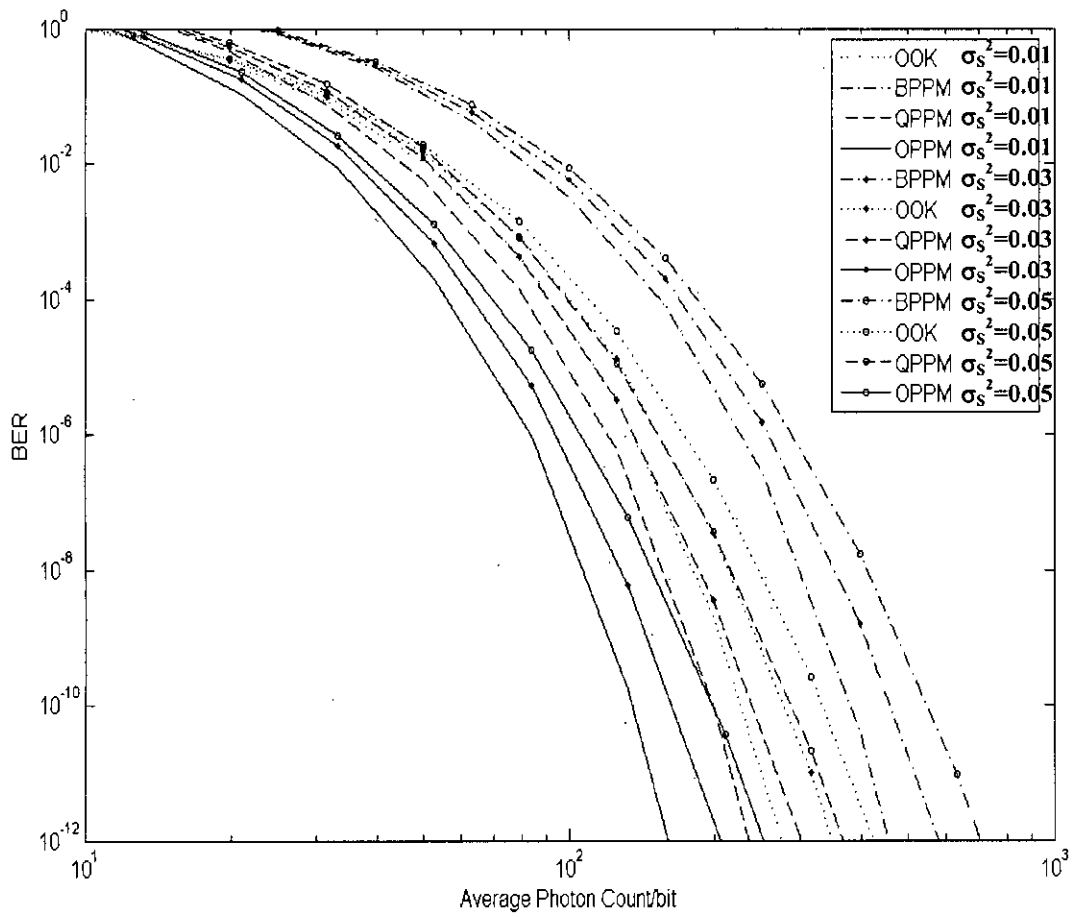


Fig. 5.8: Performance of optical OOK and M-PPM receiver in the presence of higher atmospheric scintillation

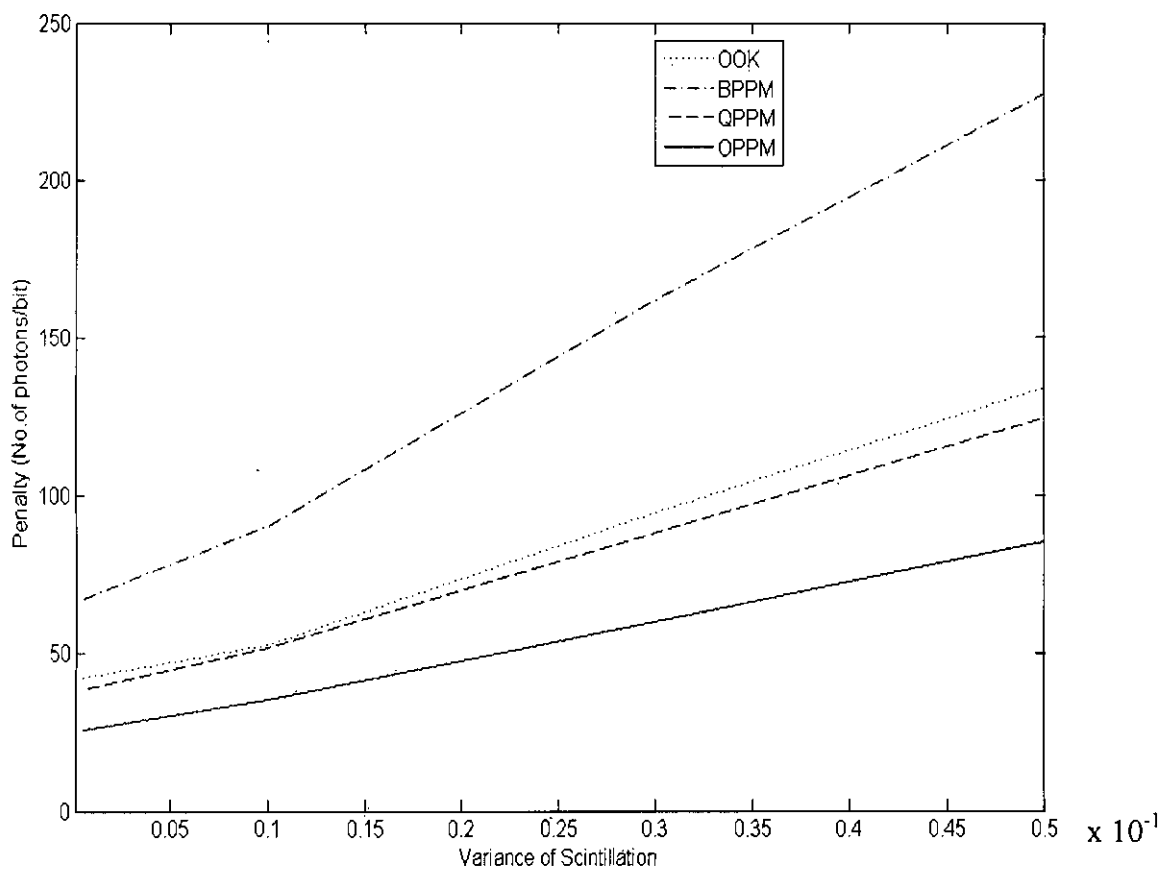


Figure 1.9: Penalty as a function of variance of scintillation

Then we evaluate the BER performance of an optical wireless link considering the multi-scattering effect for a fixed scintillation variance. The plots of BER versus average photon count per bit are shown in Fig. 5.10, 5.11, 5.12, 5.13 for OOK and M-ary PPM (M=2, 4, 8) schemes for no scattered field and for scattered fields of N=1,2,3 respectively. The curves are compared in Fig. 5.14. It is found that the deterioration in BER performance is slight due to single scattering effect and highly significant for more than one scattering fields and the system suffers penalty in receiver sensitivity to achieve a given BER. The penalty curve at a BER of 10^{-9} is shown in Fig. 5.15 as a function of number of scattered fields. It is found that penalty in unit of average photon count per bit becomes higher in multi-scattering channel than normal channel for a fixed scintillation variance. The penalty is lower for lower no of scattered fields and both the system suffered more as the no of scattered field increases. The increase of penalty to achieve a BER of 10^{-9} for a scintillation variance of 0.01 are 6.1, 10.2, 12 and 23.8 corresponding to OPPM, QPPM, OOK and BPPM respectively for N=1 and 75.5, 109.4 114, 162.5 respectively for N=2. It is also found that for N=3, both OOK and M-PPM system suffers greatly and the BER is very high which means for higher value scattering fields, normal OOK and M-PPM schemes is not acceptable and some other techniques must be needed to reduce the BER. From the above results, it is observed that OPPM suffers least amount of performance degradation compared to other modulation formats for both scintillation and multi-scattering channel effect.

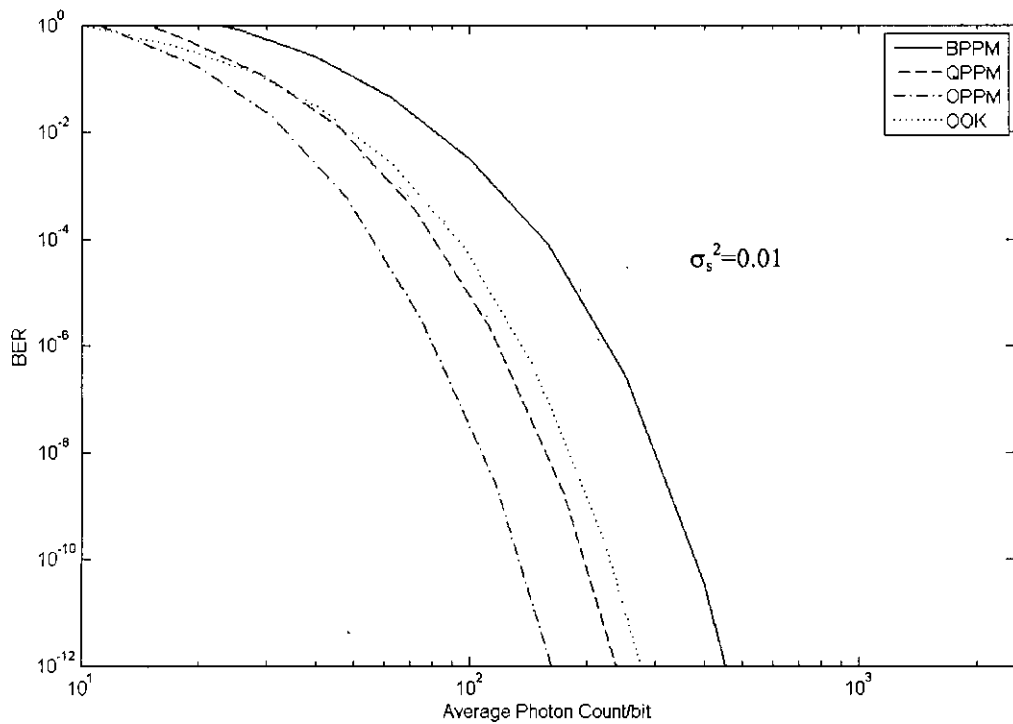


Figure 5.10: Plots of BER vs Average Photon Count/bit for no scattered fields

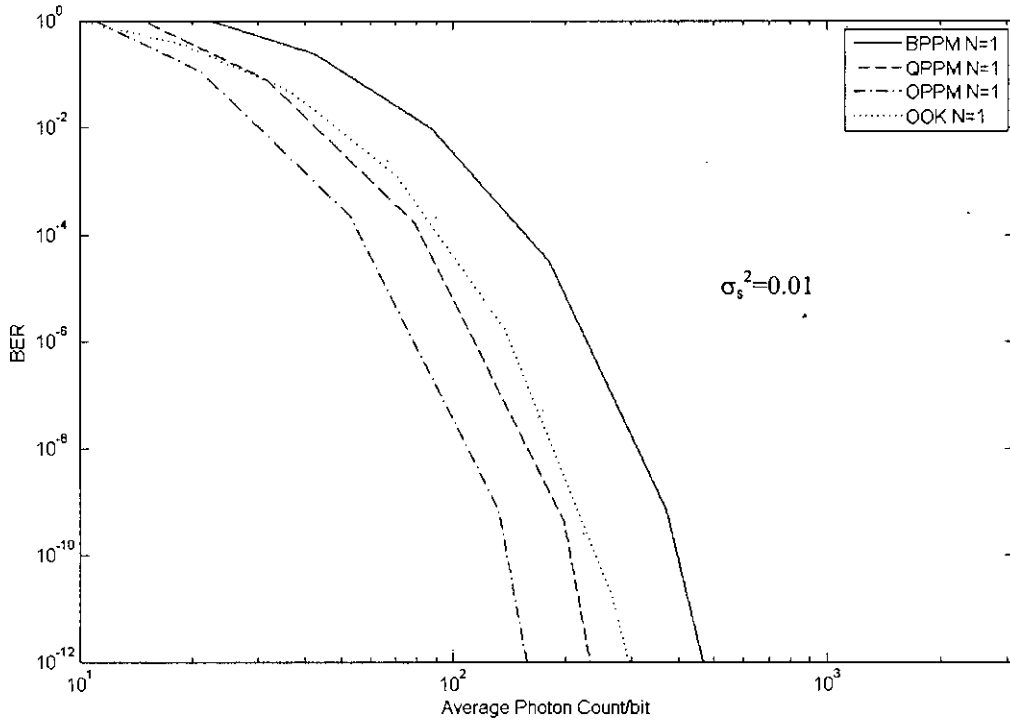


Figure 5.11: Plots of BER vs Average Photon Count/bit with scattered fields (N=1)

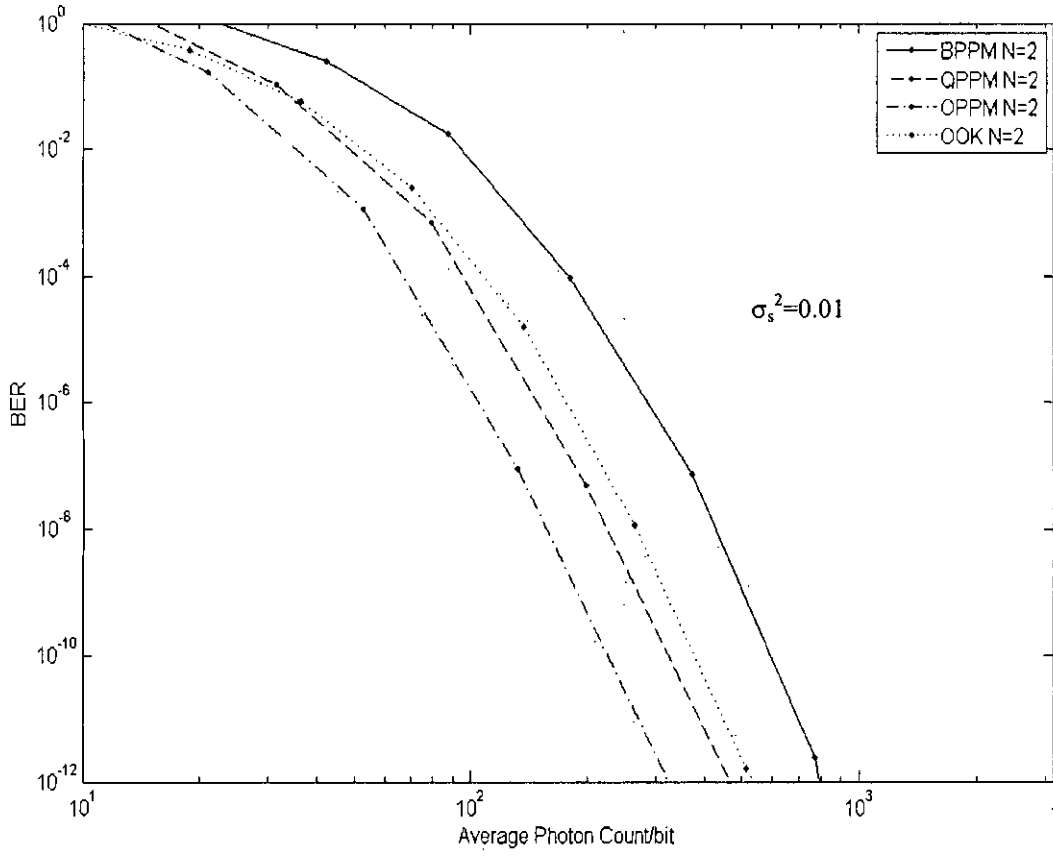


Figure 5.12 : Plots of BER vs Average Photon Count/bit with scattered fields (N=2)

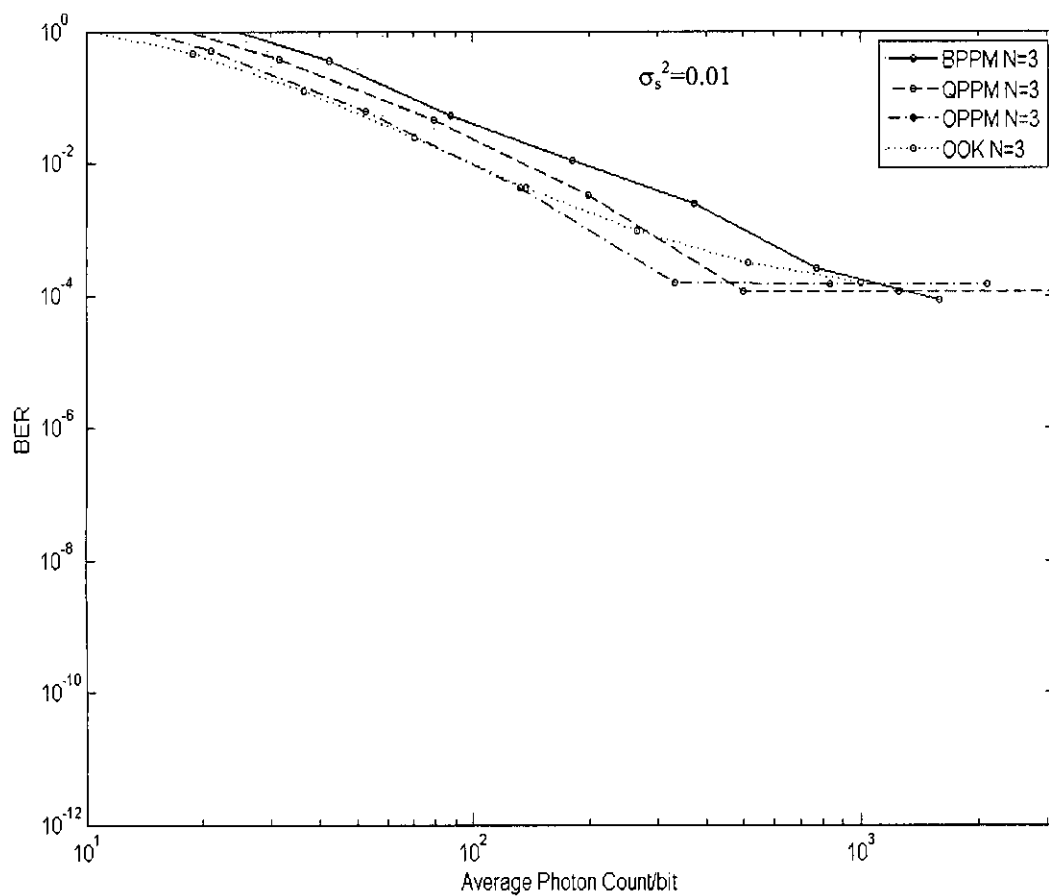


Figure 5.13: Plots of BER vs Average Photon Count/bit with scattered fields (N=3)

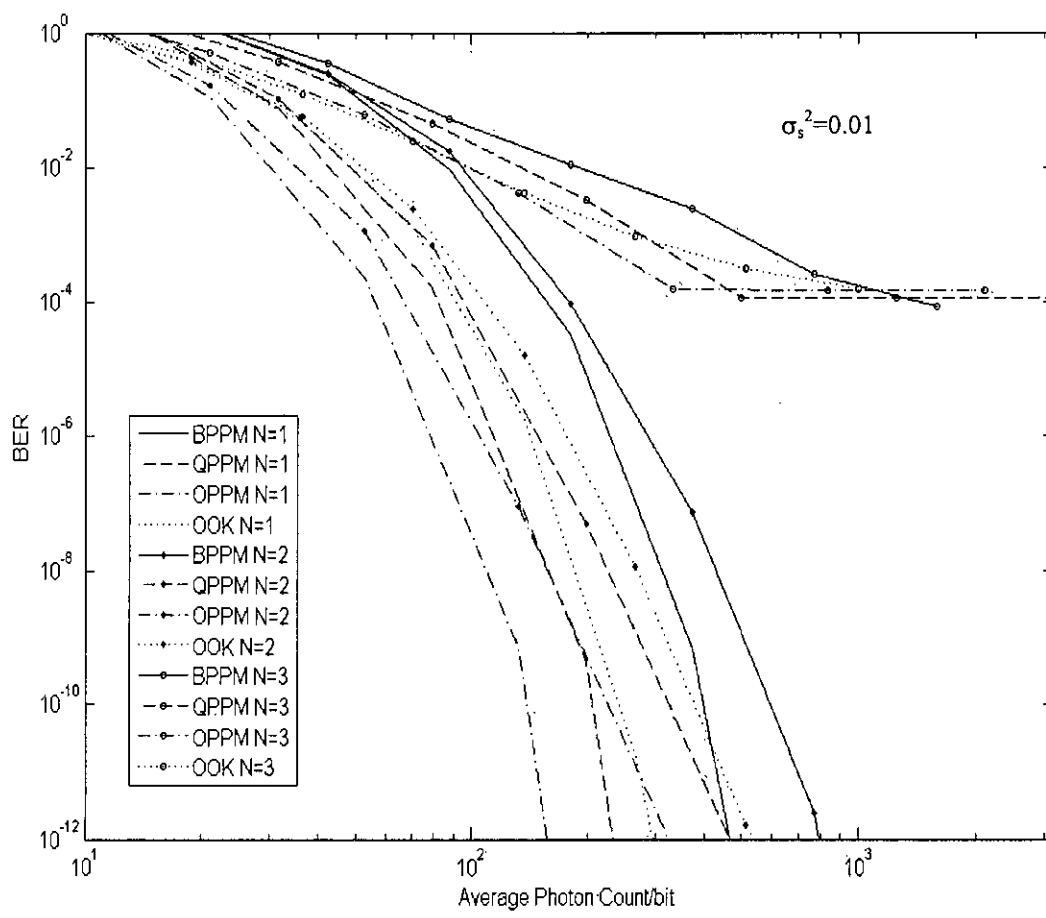


Figure 5.14: Plots of BER vs Average Photon Count/bit for different no of scattered fields

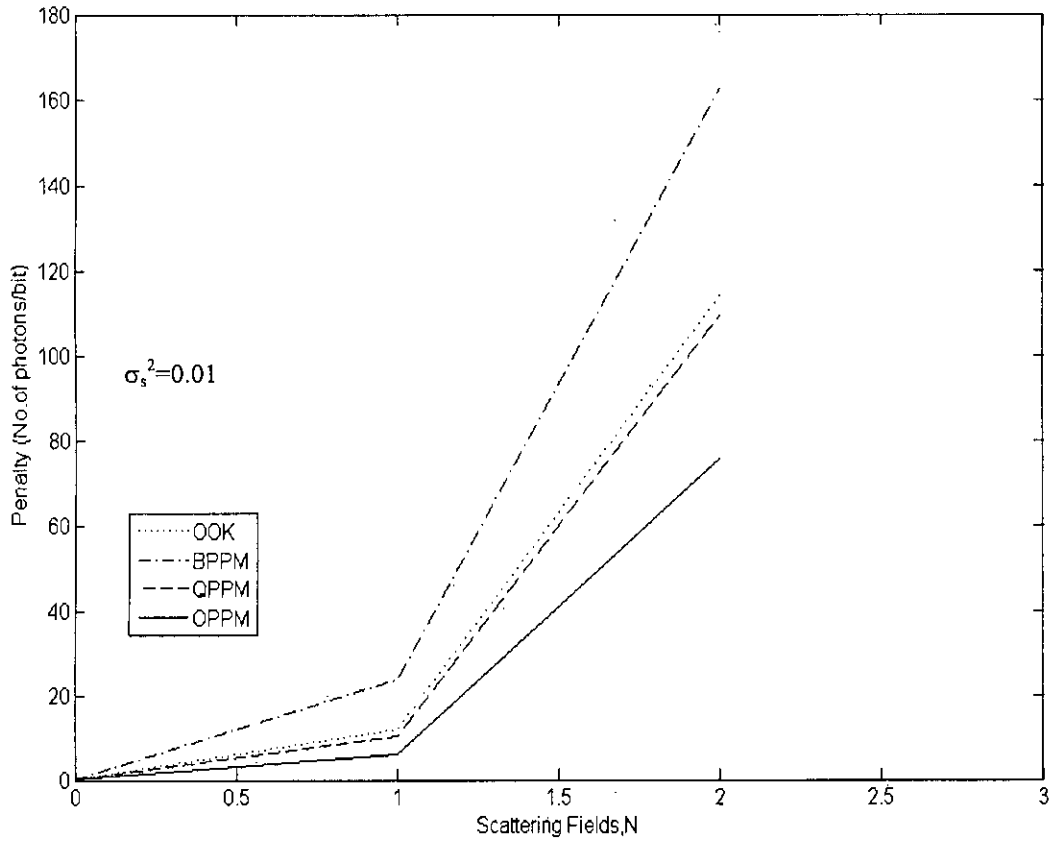


Figure 5.15: Penalty as a function of no. of scattered fields

Chapter 6

Conclusion

6.1 Conclusion

A detailed analytical approach is presented to evaluate the bit error rate performance degradation of a wireless optical link in the presence of atmospheric scintillation with OOK and M-ary PPM schemes. The analysis is extended for multi-scattering channel for a fixed value of scintillation variance.

It is found that the performance of optical direct detection OOK and M-PPM systems are very sensitive to atmospheric scintillation. There is a significant degradation in BER performance due to atmospheric scintillation and the penalty is higher for higher value of scintillation variation. It is also observed that higher order PPM offers better performance than OOK. For a fixed value of scintillation of variance, the system suffers more penalties if the channel is a multi-scattering due to the interference caused by the scattering phenomena. For lower scattered fields the systems suffered less and but as the no of scattered fields increases, both the OOK and M-PPM system suffer more. Finally, it can conclude that considering both atmospheric scintillation and mutiscattering channel higher order PPM suffers less deterioration of performance than OOK.

6.2 Further Scope of Work

Further research can be carried out on the effect of atmospheric scintillation on a WDM free-space optical link.

Research can be initiated to investigate the impact of atmospheric dispersion on a single channel and multi-channel optical free space communication system.

Further analysis can be carried out by using an optical amplifier on the system to improve the receiver sensitivity.

Forward error correction coding can be applied to minimize the effect of atmospheric scintillation and scattering and to improve the performance of a free space optical communication system.

APPENDIX A

SIMPLIFICATION OF PROBABILITY BIT ERROR RATE (BER) FOR ON OFF KEYING

The probability of bit error rate for On Off Keying (OOK) can be written as –

$$\text{Prob}_{\text{OOK}}(\text{bit error}) = \frac{1}{2\pi} \int_{D_N}^{\infty} \exp(-x^2/2) dx \quad (\text{A1})$$

$$\text{where } D_N = (\langle X_S \rangle - T_{\text{opt}}) = \frac{\langle X_S \rangle - \langle X_{ns} \rangle}{\sigma_S + \sigma_{ns}} \quad (\text{A2})$$

D_N gives the “normalized distance” between the threshold and the distribution mean. By the technique of substitution (A1) can be modified as –

$$\text{Let } z = x/\sqrt{2}$$

$$\text{Then } dz = dx/\sqrt{2}$$

$$\text{and } dx = \sqrt{2} dz$$

$$\text{As } x = D_N \Rightarrow z = \frac{D_N}{\sqrt{2}} = D_{NN}$$

$$x = \infty \Rightarrow z = \infty$$

Equation (A1) can be written as

$$\begin{aligned} \text{Prob}_{\text{OOK}}(\text{bit error}) &= \frac{1}{2\pi} \int_{D_{NN}}^{\infty} e^{-z^2} dz \cdot \sqrt{2} \\ &= \frac{1}{\pi\sqrt{2}} \int_{D_{NN}}^{\infty} e^{-z^2} dz \\ &= \frac{1}{\pi\sqrt{2}} \left[\int_{D_{NN}}^0 e^{-z^2} dz + \int_0^{\infty} e^{-z^2} dz \right] \end{aligned}$$

$$\begin{aligned}
&= \frac{1}{\pi\sqrt{2}} \left[\int_0^{\infty} e^{-z^2} dz - \int_0^{D_{NN}} e^{-z^2} dz \right] \\
&= \frac{1}{\pi\sqrt{2}} \left[\frac{\sqrt{\pi}}{2} - \frac{\sqrt{\pi}}{2} \operatorname{erf}(D_{NN}) \right] \\
&= \frac{1}{2\sqrt{2\pi}} [1 - \operatorname{erf}(D_{NN})] \\
&= \frac{1}{2\sqrt{2\pi}} \operatorname{erfc}(D_{NN}) \tag{A3}
\end{aligned}$$

where,

$$\text{error function, } \operatorname{erf}(x) = \frac{2}{\sqrt{\pi}} \int_0^x e^{-y^2} dy \tag{A4}$$

APPENDIX B

SIMPLIFICATION OF PROBABILITY BIT ERROR RATE (BER) FOR M-ARY PULSE POSITION MODULATION (MPPM)

For the Pulse Position Modulation (PPM) technique, probability of bit error rate can be written as

$$\text{Prob}_{\text{M-PPM}}(\text{bit error}) = N_{\text{BS}}(1-\text{Prob}(\text{CSC})) \quad (\text{B1})$$

where, CSC denotes "Correct Slot Choice" and

$$N_{\text{BS}} = \frac{k2^{k-1}}{(2^k - 1)} \quad (\text{B2})$$

N_{BS} is the average number of bit error per receiver error and k is the number of bits sent per word.

The probability of correct slot choice can be written as,

$$\text{Prob}(\text{CSC}) = \int_{-\infty}^{\infty} P_{X_s}(x) \left[\int_{-\infty}^{\infty} P_{X_{ns}}(y) dy \right]^{N-1} dx \quad (\text{B3})$$

Here the receiver probability densities P_{X_s} and $P_{X_{ns}}$ are normal with means $\langle X_s \rangle$ and $\langle X_{ns} \rangle$ and variances are $\sigma^2_{X_s}$ and $\sigma^2_{X_{ns}}$ respectively.

We know that probability in normal distribution is given by,

$$P(x) = \frac{1}{\sqrt{2\pi\sigma_x^2}} e^{-\frac{(x-\bar{x})^2}{2\sigma_x^2}} \quad (\text{B4})$$

\bar{x} = mean value

Equation (B3) can be written in the following form,

$$\begin{aligned}
 Prob(CSC) &= \int_{-\infty}^{\infty} P(X_s) \left[\int_{-\infty}^{X_s} P(X_{ns}) dX_{ns} \right]^{M-1} dX_s \\
 &= \int_{-\infty}^{\infty} P(X_s) \left[\int_{-\infty}^{X_s} \frac{1}{\sqrt{2\pi\sigma_{ns}}} e^{-\frac{(X_{ns}-\bar{X}_{ns})^2}{2\sigma_{ns}^2}} dX_{ns} \right]^{M-1} dX_s
 \end{aligned} \tag{B5}$$

$$\text{Let } \frac{X_{ns} - \bar{X}_{ns}}{\sqrt{2\sigma_{ns}}} = y \text{ then } dX_{ns} = \sqrt{2}\sigma_{ns} dy$$

$$\text{As, } X_{ns} = -\infty \quad \text{then } y = -\infty$$

$$X_{ns} = X_s \quad \text{then } y = \frac{X_s - \bar{X}_{ns}}{\sqrt{2}\sigma_{ns}}$$

Equation (B5) becomes,

$$\begin{aligned}
 Prob(CSC) &= \int_{-\infty}^{\infty} P(X_s) \left[\int_{-\infty}^{\frac{(X_s - \bar{X}_{ns})}{\sqrt{2}\sigma_{ns}}} \frac{1}{\sqrt{\pi}} e^{-y^2} dy \right]^{M-1} dX_s \\
 &= \int_{-\infty}^{\infty} \frac{1}{\sqrt{2\pi\sigma_s}} e^{-\frac{(X_s - \bar{X}_s)^2}{2\sigma_s^2}} \left[\int_{-\infty}^{\frac{(X_s - \bar{X}_{ns})}{\sqrt{2}\sigma_{ns}}} \frac{1}{\sqrt{\pi}} e^{-y^2} dy \right]^{M-1} dX_s
 \end{aligned} \tag{B6}$$

With the following substitution,

$$\text{Let } \frac{(X_s - \bar{X}_{ns})}{\sqrt{2}\sigma_{ns}} = z$$

$$\Rightarrow X_s = \sqrt{2}\sigma_s z + \bar{X}_s$$

$$\Rightarrow dX_s = \sqrt{2}\sigma_s dz$$

$$\text{As, } X_s = -\infty \Rightarrow z = -\infty$$

$$X_s = \infty \Rightarrow z = \infty$$

Now,

$$\begin{aligned} \frac{(X_s - \overline{X_{ns}})}{\sqrt{2}\sigma_{ns}} &= \frac{\sqrt{2}z\sigma_s + \overline{X_s} - \overline{X_{ns}}}{\sqrt{2}\sigma_{ns}} \\ &= \frac{(X_s - \overline{X_{ns}})}{\sqrt{2}\sigma_{ns}} + \frac{\sigma_s}{\sigma_{ns}} z \\ &= \delta + uz \\ &= x' \end{aligned}$$

$$\text{where, } \delta = \frac{(\overline{X_s} - \overline{X_{ns}})}{\sqrt{2}\sigma_{ns}}, \quad u = \frac{\sigma_s}{\sigma_{ns}} \quad \text{and} \quad x' = \delta + uz$$

From equation (B6)

$$\text{Prob(CSC)} = \int_{-\infty}^{\infty} \frac{1}{\sqrt{\pi}} e^{-z^2} \left[\int_{-\infty}^{x'} \frac{1}{\sqrt{\pi}} e^{-y^2} dy \right]^{M-1} dz \quad (\text{B7})$$

Now,

$$\begin{aligned} \int_{-\infty}^{x'} \frac{1}{\sqrt{\pi}} e^{-y^2} dy &= \int_{-\infty}^0 \frac{1}{\sqrt{\pi}} e^{-y^2} dy + \int_0^{x'} \frac{1}{\sqrt{\pi}} e^{-y^2} dy \\ &= \int_{-\infty}^0 \frac{1}{\sqrt{\pi}} e^{-y^2} dy + \int_0^{\infty} \frac{1}{\sqrt{\pi}} e^{-y^2} dy - \int_0^{\infty} \frac{1}{\sqrt{\pi}} e^{-y^2} dy + \int_0^{x'} \frac{1}{\sqrt{\pi}} e^{-y^2} dy \end{aligned}$$

$$\begin{aligned}
&= \int_{-\infty}^{\infty} \frac{1}{\sqrt{\pi}} e^{-y^2} dy - \int_0^{\infty} \frac{1}{\sqrt{\pi}} e^{-y^2} dy + \int_0^{x'} \frac{1}{\sqrt{\pi}} e^{-y^2} dy \\
&= 1 - \frac{1}{2} + \frac{1}{2} \operatorname{erf}(x') \\
&= 1 - \frac{1}{2} (1 - \operatorname{erf}(x')) \\
&= 1 - \frac{1}{2} \operatorname{erfc}(x')
\end{aligned}$$

$$\operatorname{Prob}(\text{CSC}) = \int_{-\infty}^{\infty} \frac{1}{\sqrt{\pi}} e^{-z^2} \left[1 - \frac{1}{2} \operatorname{erfc}(x')\right]^{M-1} dz \quad (\text{B8})$$

For M=2

$$\begin{aligned}
\operatorname{Prob}(\text{CSC}) &= \int_{-\infty}^{\infty} \frac{1}{\sqrt{\pi}} e^{-z^2} \left[1 - \frac{1}{2} \operatorname{erfc}(x')\right]^1 dz \\
&= \int_{-\infty}^{\infty} \frac{1}{\sqrt{\pi}} e^{-z^2} dz - \frac{1}{2} \int_{-\infty}^{\infty} \frac{1}{\sqrt{\pi}} e^{-z^2} \operatorname{erfc}(x') dz \\
&= 1 - \frac{1}{2} \int_{-\infty}^{\infty} \frac{1}{\sqrt{\pi}} e^{-z^2} \operatorname{erfc}(x') dz \quad (\text{B9})
\end{aligned}$$

$$\operatorname{Prob}_{M\text{-PPM}}(\text{bit error}) = N_{BS} (1 - \operatorname{Prob}(\text{CSC}))$$

$$= \frac{N_{BS}}{2\sqrt{\pi}} \int_{-\infty}^{\infty} e^{-z^2} \operatorname{erfc}(x') dz \quad (\text{B10})$$

For M=4

$$\begin{aligned}
 \text{Prob(CSC)} &= \int_{-\infty}^{\infty} \frac{1}{\sqrt{\pi}} e^{-z^2} \left[1 - \frac{1}{2} \text{erfc}(x')\right]^3 dz \\
 &= \int_{-\infty}^{\infty} \frac{1}{\sqrt{\pi}} e^{-z^2} \left[1 - \frac{3}{2} \text{erfc}(x') + \frac{3}{4} (\text{erfc}(x'))^2 - \frac{1}{8} (\text{erfc}(x'))^3\right] dz \\
 &= \int_{-\infty}^{\infty} \frac{1}{\sqrt{\pi}} e^{-z^2} - \frac{1}{2\sqrt{\pi}} \int_{-\infty}^{\infty} e^{-z^2} (3\text{erfc}(x') - \frac{3}{2} (\text{erfc}(x'))^2 + \frac{1}{4} (\text{erfc}(x'))^3) dz \\
 &= 1 - \frac{1}{2\sqrt{\pi}} \int_{-\infty}^{\infty} e^{-z^2} (3\text{erfc}(x') - \frac{3}{2} (\text{erfc}(x'))^2 + \frac{1}{4} (\text{erfc}(x'))^3) dz \quad (\text{B16})
 \end{aligned}$$

Therefore,

$$\begin{aligned}
 \text{Prob}_{M\text{-ppM}}(\text{bit error}) &= N_{BS} (1 - \text{Prob(CSC)}) \\
 &= \frac{N_{BS}}{2\sqrt{\pi}} \int_{-\infty}^{\infty} e^{-z^2} (3\text{erfc}(x') - \frac{3}{2} (\text{erfc}(x'))^2 + \frac{1}{4} (\text{erfc}(x'))^3) dz \quad (\text{B17})
 \end{aligned}$$

For M=8

$$\begin{aligned}
 \text{Prob(CSC)} &= \int_{-\infty}^{\infty} \frac{1}{\sqrt{\pi}} e^{-z^2} \left[1 - \frac{1}{2} \text{erfc}(x')\right]^7 dz \\
 &= \int_{-\infty}^{\infty} \frac{1}{\sqrt{\pi}} e^{-z^2} \left[1 - \frac{7}{2} \text{erfc}(x') + \frac{21}{4} (\text{erfc}(x'))^2 - \frac{35}{8} (\text{erfc}(x'))^3 + \frac{35}{16} (\text{erfc}(x'))^4 \right. \\
 &\quad \left. - \frac{21}{32} (\text{erfc}(x'))^5 + \frac{7}{64} (\text{erfc}(x'))^6 - \frac{7}{128} (\text{erfc}(x'))^7\right] dz \quad (\text{B18})
 \end{aligned}$$

Therefore,

$$\begin{aligned}
\text{Prob}(CSC) &= \int_{-\infty}^{\infty} \frac{1}{\sqrt{\pi}} e^{-z^2} dz - \frac{1}{2\sqrt{\pi}} \int_{-\infty}^{\infty} e^{-z^2} \left[7\text{erfc}(x') - \frac{21}{2}(\text{erfc}(x'))^2 + \frac{35}{4}(\text{erfc}(x'))^3 \right. \\
&\quad \left. - \frac{35}{8}(\text{erfc}(x'))^4 + \frac{21}{16}(\text{erfc}(x'))^5 - \frac{7}{32}(\text{erfc}(x'))^6 + \frac{1}{64}(\text{erfc}(x'))^7 \right] dz \\
&= 1 - \frac{1}{2\sqrt{\pi}} \int_{-\infty}^{\infty} e^{-z^2} \left[7\text{erfc}(x') - \frac{21}{2}(\text{erfc}(x'))^2 + \frac{35}{4}(\text{erfc}(x'))^3 - \frac{35}{8}(\text{erfc}(x'))^4 \right. \\
&\quad \left. + \frac{21}{16}(\text{erfc}(x'))^5 - \frac{7}{32}(\text{erfc}(x'))^6 + \frac{1}{64}(\text{erfc}(x'))^7 \right] dz \quad (B19)
\end{aligned}$$

APPENDIX C

HERMITE POLYNOMIAL

Hermite polynomial for orthogonal is given by

$$H_n(x) = \int_{-\infty}^{\infty} e^{-x^2} f(x) dx = \sum_{i=1}^n w_i f(x_i) + R_n$$

Abscissas: x_i is the i^{th} zero of $H_n(x)$.

Weights:

$$\frac{2^{n-1} n! \sqrt{\pi}}{n^2 [H_{n-1}(x_i)]^2}$$

Remainder:

$$R_n = \frac{n! \sqrt{\pi}}{2^n (2n)!} f^{(2n)}(\epsilon) \quad (-\infty < \epsilon < \infty)$$

ABSCISSAS AND WEIGHT FACTORS FOR HERMITE INTEGRATION

$$\int_{-\infty}^{\infty} e^{-x^2} f(x) dx = \sum_{i=1}^n w_i f(x_i)$$

Abscissas = x_i ; (Zeros of Hermite Polynomials)

$$\int_{-\infty}^{\infty} g(x) dx = \sum_{i=1}^n w_i e^{x_i^2} g(x_i)$$

Weight Factors = w_i

x_i	w_i	$w_i e^{x_i^2}$
n=2		
0.70710 67811 86548	(-1) 8.86226 92545 28	1.46114 11826 611
n=3		
0.00000 00000 00000	(0) 1.18163 59006 04	1.18163 59006 037
1.22474 48713 91589	(-1) 2.95408 97515 09	1.32393 11752 136
n=4		
0.52464 76232 75290	(-1) 8.04914 09000 55	1.05996 44828 950
1.65068 01238 85785	(-2) 8.13128 35447 25	1.24022 58176 958
n=5		
0.00000 00000 00000	(-1) 9.45308 72048 29	0.94530 87204 829
0.95857 24646 13819	(-1) 3.93619 32315 22	0.98658 09967 514
2.02018 28704 56086	(-2) 1.99532 42059 05	1.18148 66255 350
n=6		
0.43607 74119 27617	(-1) 7.24629 59522 44	0.87640 13344 362
1.33584 90740 13697	(-1) 1.57067 32032 29	0.93558 05576 312
2.35060 49736 74492	(-3) 4.53000 99055 09	1.13690 83326 745
n=7		
0.00000 00000 00000	(-1) 8.10264 61755 68	0.81026 46175 568
0.81628 78828 58965	(-1) 4.25607 25261 01	0.82868 73032 836
1.67355 16287 67471	(-2) 5.45155 82819 13	0.89718 46002 252
2.65196 13568 35233	(-4) 9.71781 24509 95	1.10133 07296 103
n=8		
0.38118 69902 07322	(-1) 6.61147 01255 82	0.76454 41286 517
1.15719 37124 46780	(-1) 2.07802 32581 49	0.79289 00403 864
1.98165 67566 95843	(-2) 1.70779 83007 41	0.86675 26065 634
2.93063 74202 57244	(-4) 1.99604 07221 14	1.07193 01442 480
n=9		
0.00000 00000 00000	(-1) 7.20235 21560 61	0.72023 52156 061
0.72355 10187 52838	(-1) 4.32651 55900 26	0.73030 24527 451
1.46855 32892 16668	(-2) 8.84745 27394 38	0.76460 81250 946
2.26658 05845 31843	(-3) 4.94362 42755 37	0.84175 27014 787
3.19099 32017 81528	(-5) 3.96069 77263 26	1.04700 35809 767

x_i	w_i	$w_i e^{x_i^2}$
n=10		
0.34290 13272 23705	(-1) 6.10862 63373 53	0.68708 18539 513
1.03661 08297 89514	(-1) 2.40136 61108 23	0.70329 63231 049
1.75868 36492 99882	(-2) 3.38743 94455 48	0.74144 19319 436
2.53273 16742 32790	(-3) 1.54364 57467 81	0.82066 61264 048
3.43615 91188 37738	(-6) 7.64043 28552 33	1.02545 16913 657
n=12		
0.31424 03762 54359	(-1) 5.70135 23626 25	0.62930 78743 695
0.94778 83912 40164	(-1) 2.60492 31026 42	0.63962 12320 203
1.59768 26351 52605	(-2) 5.16079 85615 88	0.66266 27732 669
2.27950 70805 01060	(-3) 3.90539 05846 29	0.70522 03661 122
3.02063 70251 20890	(-5) 8.57368 70435 88	0.78664 39394 633
3.88972 48978 69782	(-7) 2.65855 16843 56	0.98969 90470 923
n=16		
0.27348 10461 3815	(-1) 5.07929 47901 66	0.54737 52050 378
0.82295 14491 4466	(-1) 2.80647 45052 85	0.55244 19573 675
1.38025 85391 9888	(-2) 8.38100 41398 99	0.56321 78290 882
1.95178 79909 1625	(-2) 1.20883 11535 51	0.58124 72754 009
2.54620 21578 4748	(-4) 9.32284 00862 42	0.60973 69582 560
3.17699 91619 7996	(-5) 2.71186 00925 38	0.65575 56728 761
3.86944 79048 6012	(-7) 2.32098 08448 65	0.73824 56222 777
4.68873 89393 0582	(-10) 2.65480 74740 11	0.93687 44928 841
n=20		
0.24534 07083 009	(-1) 4.62243 66960 06	0.49092 15006 667
0.73747 37285 454	(-1) 2.86675 50536 28	0.49384 33852 721
1.23407 62153 953	(-1) 1.09017 20602 00	0.49992 08713 363
1.73853 77121 166	(-2) 2.48105 20687 46	0.50967 90271 175
2.25497 40020 893	(-3) 3.24377 33422 38	0.52408 03509 486
2.78880 60584 281	(-4) 2.28338 63601 63	0.54485 17423 644
3.34785 45673 832	(-6) 7.80255 64785 32	0.57526 24428 525
3.94476 40401 156	(-7) 1.08606 93707 69	0.62227 86961 914
4.60368 24495 507	(-10) 4.39934 09922 73	0.70433 29611 769
5.38748 08900 112	(-13) 2.22939 36455 34	0.89859 19614 532

